effects than PEG-IFN-α2b. In addition, IFNAR-2 expression in the tumor of mice decreased, particularly in mice that received PEG-IFN-α2b. This was considered to be due to IFNAR-2 expression being down-regulated as a result of the long-term continuous action of PEG-IFN-α2b, and this is consistent with the *in vitro* findings. The above indicates that even if IFNAR-2 expression is down-regulated, antitumor effect does not decrease but, in fact, increases due to continuous action. In contrast, Krepler et al. (41) compared antitumor effects of PEG-IFN-α2a and non-PEG-IFN-α2a in a human melanoma SCID mouse xenotransplantation model and found no significant differences in tumor growth inhibition. We presume that this opposite result is attributable to the difference in the experimental conditions. For example, in their study, mice received extremely high doses of PEG- and non-PEG-IFN-α2a, i.e., mice received 900 μg of PEG-IFN-α2a (45 000 μg/kg) that is five or 10 times larger than the clinical dose for chronic hepatitis C patients (90–180 μg/body, 1.8–3.6 μg/kg). In addition, it is not clear whether the amounts of PEG- and non-PEG-IFN-α2a administrated to mice were equivalent in antiproliferative effects on the melanoma cells *in vitro*.

The induction of apoptosis is known as a mechanism of the *in vivo* antiproliferation activity of PEG-IFN-α2b. However, the induction of S-phase arrest that was observed *in vitro* was not clear *in vivo* in terms of the labeling index of BrdU. This was the same as the finding on the mechanism of the antiproliferation activity of IFN-αCon1 in mouse tumor (12). It is surmized that apoptosis holds the dominant position over the S-phase arrest when tumor cells *in vivo* were treated with IFN-α for 2 weeks. This point should be further investigated. Antiangiogenesis activity is one of the biological effects of IFN-α, and the administration of IFN-α to patients with vascular tumors, e.g., Kaposi sarcoma, results in the significant regression of tumor lesions (1, 4). IFN administration suppresses the growth of human tumor that was transplanted to mice through an antiangiogenesis effect (12, 31, 42–45). Tedjarati et al. (44) found that once per week injection of 7000 IU of PEG-IFN-α2b into nude mice bearing ip growing human ovarian carcinoma cells inhibited angiogenesis and tumor growth and that PEG-IFN-α2b administered at higher or lower doses was less effective. In our current study, however, significant antiangiogenesis effect was not observed at any dose. In another study that we conducted examining a consecutive 14-day administration of 5000 IU/mouse/day of BALL-1 IFN-α to mice that had subcutaneous transplantation of HAK-1B tumor, a slight increase in the number of blood vessels and an increase of the three angiogenesis factors were observed (46). On the other hand, another study that used 0.01 or 0.1 μg/mouse of IFN-αCon1 showed a significant decrease in the number of blood vessels (12). Further studies are necessary both *in vitro* and *in vivo* with various IFNs such as IFN-α and IFN-β to clarify whether the antiangiogenesis effects are attributable to the type of IFN. In addition, more studies are also needed to investigate the mechanism of antiproliferative effects including antiangiogenesis, the expression of IFNAR-2 and its relationship to antiproliferative effects using other HCC cells.

In the HCC cell line HAK-1B, continuous contact with PEG-IFN-α2b induced the down-regulation of IFNAR-2 and a potent antiproliferative effect that is stronger than the effects of non-PEG-IFN-α2b. The antitumor effect of PEG-IFN-α2b was expressed at approximately 1/3 of the clinical dose, and this suggests that PEG-IFN-α2b administration to patients with chronic hepatitis C would be effective in the prevention of hepatocarcinogenesis and the recurrence of HCC.

Acknowledgements

We thank Ms. Akemi Fujiyoshi and Dr. Akiko Takayama for their assistance in our experiments. This study was supported in part by the Sarah Cousins Memorial Fund, Boston, Massachusetts, and by a Grant-in-Aid from the Ministry of Health, Labor and Welfare of Japan (#17200501).

References

1. Stark G R, Kerr I M, Williams B R, Silverman R H, Schreiber R D. How cells respond to interferons. Annu Rev Biochem 1998; 67: 227–64.
2. Xu D, Erickson S, Szeps M, et al. Interferon α down-regulates telomerase reverse transcriptase and telomerase activity in human malignant and nonmalignant hematopoietic cells. Blood 2000; 96: 4313–8.
3. Pestka S, Langer J A, Zoon K C, Samuel C E. Interferons and their actions. Annu Rev Biochem 1987; 56: 727–77.
4. Gutterman J U. Cytokine therapeutics: lessons from interferon α. Proc Natl Acad Sci USA 1994; 91: 1198–205.
5. Ikeda K, Saitoh S, Arase Y, et al. Effect of interferon therapy on hepatocellular carcinogenesis in patients with chronic hepatitis type C: a long-term observation study of 1643 patients using statistical bias correction with proportional hazard analysis. Hepatology 1999; 29: 1124–30.
6. Ikeda K, Arase Y, Saitoh S, et al. Interferon beta prevents recurrence of hepatocellular carcinoma after complete resection or ablation of the primary tumor-A prospective randomized study of hepatitis C virus-related liver cancer. Hepatology 2000; 32: 228–32.
7. Mazzella G, Accogli E, Sottili S, et al. Alpha interferon treatment may prevent hepatocellular carcinoma in HCV-related liver cirrhosis. J Hepatol 1996; 24: 141–7.

8. Nishiguchi S, Kuroki T, Nakatani S, et al. Randomised trial of effects of interferon-α on incidence of hepatocellular carcinoma in chronic active hepatitis C with cirrhosis. Lancet 1995; 346: 1051–5.
9. Nishiguchi S, Tamori A, Kubo S. Effect of long-term postoperative interferon therapy on intrahepatic recurrence and survival rate after resection of hepatitis C virus-related hepatocellular carcinoma. Intervirology 2005; 48: 71–5.
10. Sakaguchi Y, Kudo M, Fukunaga T, Minami Y, Chung H, Kawasaki T. Low-dose, long-term, intermittent interferon-alpha-2b therapy after radical treatment by radiofrequency ablation delays clinical recurrence in patients with hepatitis C virus-related hepatocellular carcinoma. Intervirology 2005; 48: 64–70.
11. Yano H, Iemura A, Haramaki M, et al. Interferon alfa receptor expression and growth inhibition by interferon alfa in human liver cancer cell lines. Hepatology 1999; 29: 1708–17.
12. Hisaka T, Yano H, Ogasawara S, et al. Interferon-αCon1 suppresses proliferation of liver cancer cell lines *in vitro* and *in vivo*. J Hepatol 2004; 41: 782–9.
13. Negrier S, Escudier B, Lasset C, et al. Recombinant human interleukin-2, recombinant human interferon alfa-2a, or both in metastatic renal-cell carcinoma. Groupe Francais d'Immunotherapie. N Engl J Med 1998; 338: 1272–8.
14. Sakon M, Nagano H, Dono K, et al. Combined intraarterial 5-fluorouracil and subcutaneous interferon-alpha therapy for advanced hepatocellular carcinoma with tumor thrombi in the major portal branches. Cancer 2002; 94: 435–42.
15. Baker D E. Pegylated interferon plus ribavirin for the treatment of chronic hepatitis C. Rev Gastroenterol Disord 2003; 3: 93–109.
16. Reddy K R, Wright T L, Pockros P J, et al. Efficacy and safety of pegylated (40-kd) interferon α-2a compared with interferon α-2a in noncirrhotic patients with chronic hepatitis C. Hepatology 2001; 33: 433–8.
17. Lindsay K L, Trepo C, Heintges T, et al. A randomized, double-blind trial comparing pegylated interferon alfa-2b to interferon alfa-2b as initial treatment for chronic hepatitis C. Hepatology 2001; 34: 395–403.
18. Craxi A, Licata A. Clinical trial results of peginterferons in combination with ribavirin. Semin Liver Dis 2003; 23(Suppl. 1): 35–46.
19. Lee S D, Yu M L, Cheng P N, et al. Comparison of a 6-month course peginterferon α-2b plus ribavirin and interferon α-2b plus ribavirin in treating Chinese patients with chronic hepatitis C in Taiwan. J Viral Hepatol 2005; 12: 283–91.
20. Bruno S, Camma C, Di Marco V, et al. Peginterferon alfa-2b plus ribavirin for naive patients with genotype 1 chronic hepatitis C: a randomized controlled trial. J Hepatol 2004; 41: 474–81.
21. Utsunomiya I, Iemura A, Yano H, Akiba J, Kojiro M. Establishment and characterization of a new human hepatocellular carcinoma cell line, HAK-3, and its response to growth factors. Int J Oncol 1999; 15: 669–75.
22. Murakami T. Establishment and characterization of human hepatoma cell line (KIM-1). Acta Hepatol Jpn 1984; 25: 532–9.
23. Murakami T, Maruiwa M, Fukuda K, Kojiro M, Tanaka M, Tanikawa K. Characterization of a new human hepatoma cell line (KYN-3) derived from the ascites of the hepatoma patient [Abstract]. Jpn J Cancer Res 1988;Proceedings of the Japanese Cancer Association: 292.
24. Murakami T, Yano H, Maruiwa M, Sugihara S, Kojiro M. Establishment and characterization of a human combined hepatocholangiocarcinoma cell line and its heterologous transplantation in nude mice. Hepatology 1987; 7: 551–6.
25. Haramaki M, Yano H, Iemura A, et al. A new human hepatocellular carcinoma cell line (HAK-2) forms various structures in collagen gel matrices. Hum Cell 1997; 10: 183–92.
26. Yano H, Iemura A, Fukuda K, Mizoguchi A, Haramaki M, Kojiro M. Establishment of two distinct human hepatocellular carcinoma cell lines from a single nodule showing clonal dedifferentiation of cancer cells. Hepatology 1993; 18: 320–7.
27. Yano H, Iemura A, Haramaki M, et al. A human combined hepatocellular and cholangiocarcinoma cell line (KMCH-2) that shows the features of hepatocellular carcinoma or cholangiocarcinoma under different growth conditions. J Hepatol 1996; 24: 413–22.
28. Yano H, Kojiro M, Nakashima T. A new human hepatocellular carcinoma cell line (KYN-1) with a transformation to adenocarcinoma. In Vitro Cell Dev Biol 1986; 22: 637–46.
29. Yano H, Maruiwa M, Murakami T, et al. A new human pleomorphic hepatocellular carcinoma cell line, KYN-2. Acta Pathol Jpn 1988; 38: 953–66.
30. Nakanishi K, Maruyama M, Shibata T, Morishima N. Identification of a caspase-9 substrate and detection of its cleavage in programmed cell death during mouse development. J Biol Chem 2001; 276: 41237–44.
31. Takemoto Y, Yano H, Momosaki S, et al. Antiproliferative effects of interferon-αCon1 on ovarian clear cell adenocarcinoma *in vitro* and *in vivo*. Clin Cancer Res 2004; 10: 7418–26.
32. Yano H, Yanai Y, Momosaki S, et al. Growth inhibitory effects of interferon-α subtypes vary according to human liver cancer cell lines. J Gastroenterol Hepatol 2006, in press.
33. Evans T, Secher D. Kinetics of internalisation and degradation of surface-bound interferon in human lymphoblastoid cells. EMBO J 1984; 3: 2975–8.
34. Zoon K C, Zur Nedden D, Hu R, Arnheiter H. Analysis of the steady state binding, internalization, and degradation of human interferon-α2. J Biol Chem 1986; 261: 4993–6.
35. Lau J Y, Sheron N, Morris A G, Bomford A B, Alexander G J, Williams R. Interferon-α receptor expression and regulation in chronic hepatitis B virus infection. Hepatology 1991; 13: 332–8.
36. Nakajima S, Kuroki T, Shintani M, et al. Changes in interferon receptors on peripheral blood mononuclear cells from patients with chronic hepatitis B being treated with interferon. Hepatology 1990; 12: 1261–5.
37. Tochizawa S, Akamatsu S, Sugiyama Y, et al. A flow cytometric method for determination of the interferon receptor IFNAR2 subunit in peripheral blood leukocyte subsets. J Pharmacol Toxicol Methods 2004; 50: 59–66.
38. Lutfalla G, Holland S J, Cinato E, et al. Mutant U5A cells are complemented by an interferon-αβ receptor subunit generated by alternative processing of a new member of a cytokine receptor gene cluster. EMBO J 1995; 14: 5100–8.
39. Domanski P, Witte M, Kellum M, et al. Cloning and expression of a long form of the β subunit of the interferon αβ receptor that is required for signaling. J Biol Chem 1995; 270: 21606–11.
40. Dooley J S, Vergalla J, Hoofnagle J H, Zoon K C, Munson P J, Jones E A. Specific binding of human alpha interferon to high-affinity cell-surface binding sites on peripheral blood mononuclear cells. J Lab Clin Med 1989; 113: 623–31.
41. Krepler C, Certa U, Wacheck V, Jansen B, Wolff K, Pehamberger H. Pegylated and conventional interferon-α

induce comparable transcriptional responses and inhibition of tumor growth in a human melanoma SCID mouse xenotransplantation model. J Invest Dermatol 2004; 123: 664–9.
42. Dinney C P, Bielenberg D R, Perrotte P, et al. Inhibition of basic fibroblast growth factor expression, angiogenesis, and growth of human bladder carcinoma in mice by systemic interferon-alpha administration. Cancer Res 1998; 58: 808–14.
43. Hong Y K, Chung D S, Joe Y A, et al. Efficient inhibition of *in vivo* human malignant glioma growth and angiogenesis by interferon-beta treatment at early stage of tumor development. Clin Cancer Res 2000; 6: 3354–60.
44. Tedjarati S, Baker C H, Apte S, et al. Synergistic therapy of human ovarian carcinoma implanted orthotopically in nude mice by optimal biological dose of pegylated interferon alpha combined with paclitaxel. Clin Cancer Res 2002; 8: 2413–22.
45. Singh R K, Gutman M, Llansa N, Fidler I J. Interferon-beta prevents the upregulation of interleukin-8 expression in human melanoma cells. J Interferon Cytokine Res 1996; 16: 577–84.
46. Kojiro S, Yano H, Ogasawara S, et al. Antiproliferative effects of 5-fluorouracil and interferon-alpha in combination on a hepatocellular carcinoma cell line *in vitro* and *in vivo*. J Gastroenterol Hepatol 2006; 21: 129–37.

THE JOURNAL OF BIOLOGICAL CHEMISTRY VOL. 281, NO. 52, pp. 40440–40449, December 29, 2006

YB-1 Is Important for an Early Stage Embryonic Development

NEURAL TUBE FORMATION AND CELL PROLIFERATION[*S]

Received for publication, June 21, 2006, and in revised form, October 13, 2006 Published, JBC Papers in Press, November 2, 2006, DOI 10.1074/jbc.M605948200

Takeshi Uchiumi[‡1], Abbas Fotovati[§], Takakazu Sasaguri[¶], Kohtaro Shibahara[‖], Tatsuo Shimada[**], Takao Fukuda[‖], Takanori Nakamura[‖], Hiroto Izumi[‡], Teruhisa Tsuzuki[‡‡], Michihiko Kuwano[§], and Kimitoshi Kohno[‡]

From the [‡]Department of Molecular Biology, University of Occupational and Environmental Health, School of Medicine, Yahatanishi-ku, Kitakyushu 807-8555, [§]Research Center for Innovative Cancer Therapy, Kurume University, Kurume, Fukuoka 830-0011, the [¶]Department of Pathology II, University of Occupational and Environmental Health, School of Medicine, Yahatanishi-ku, Kitakyushu 807-8555, the [‖]Department of Medical Biochemistry, Graduate School of Medical Sciences, Kyushu University, Fukuoka 812-8582, [**]Health Sciences, School of Nursing, Faculty of Medicine, Oita University, Yufushi 879-5595, and [‡‡]Medical Biophysics and Radiation Biology, Graduate School of Medical Sciences, Kyushu University, Fukuoka 812-8582, Japan

The eukaryotic Y-box-binding protein-1 (YB-1) is involved in the transcriptional and translational control of many biological processes, including cell proliferation. In clinical studies, the cellular level of YB-1 closely correlates with tumor growth and prognosis. To understand the role of YB-1 *in vivo*, especially in the developmental process, we generated YB-1 knock-out mice, which are embryonic lethal and exhibit exencephaly associated with abnormal patterns of cell proliferation within the neuroepithelium. β-Actin expression and F-actin formation were reduced in the *YB-1* null embryo and *YB-1*$^{-/-}$ mouse embryonic fibroblasts, suggesting that the neural tube defect is caused by abnormal cell morphology and actin assembly within the neuroepithelium. Fibroblasts derived from *YB-1*$^{-/-}$ embryos demonstrated reduced growth and cell density. A colony formation assay showed that *YB-1*$^{-/-}$ mouse embryonic fibroblasts failed to undergo morphological transformation and remained contact-inhibited in culture. These results demonstrate that YB-1 is involved in early mouse development, including neural tube closure and cell proliferation.

The Y-box protein family is characterized by a highly conserved cold-shock domain that binds nucleic acids and shares homology with the prokaryotic cold-shock proteins (1, 2). The human Y-box-binding gene, *YB-1*, is located on chromosome 1p34 (1). YB-1 has multiple functions but was initially identified as a transcription factor that associates with the Y-box sequence of the major histocompatibility complex class II genes (3).

YB-1 promotes cell proliferation through its transcriptional regulation of target genes such as proliferating cell nuclear antigen (PCNA),[2] epidermal growth factor receptor, DNA topoisomerase IIα, thymidine kinase, and DNA polymerase α (4, 5). We previously reported its role in the transcriptional activation of human multidrug resistance 1 (*MDR1*) and DNA topoisomerase IIα in response to various environmental stimuli (6, 7). In addition, it has been shown to chaperone RNA, modify chromatin, participate in the translational masking of mRNA, and be involved in stress responses such as the redox signaling pathway (8). Eukaryotic Y-box proteins also regulate gene expression at the translational level through their recognition of RNA (9–11), and therefore play critical roles in both mRNA turnover and translational control.

YB-1 protects mammalian cells from the cytotoxic effects induced by DNA damage. We previously reported that human cancer cell lines overexpressing YB-1 resist cisplatin, whereas the reduction of YB-1 itself leads to increased sensitivity to cisplatin, other DNA-interacting drugs, and UV irradiation (2). YB-1 is mainly localized in the cytoplasm, but translocates to the nucleus following UV irradiation of cells or treatment with anticancer drugs (12). YB-1 binds directly to repair-associated proteins such as PCNA and p53 (13), whereas proteolytic cleavage of the C-terminal fragment is linked to stress induced by DNA damage (14).

In clinical studies, the cellular level of YB-1 has been shown to correlate with tumor growth and prognosis in cancers of the ovary, lung, and breast (15). Moreover, overexpression or the nuclear presence or absence of YB-1 plays a critical role in P-glycoprotein expression, malignant progression, poor prognosis, and global drug resistance (2, 15, 16).

To understand how YB-1 proteins exert their multiple functions, we previously established mouse embryonic stem cell lines with a heterozygously targeted disruption of the *YB-1* gene (*YB-1*$^{+/-}$), and we demonstrated their hypersensitivity to cytotoxic agents such as cisplatin and mitomycin C (17).

Here we carried out targeted disruptions of the mouse *YB-1* gene to elucidate the role of YB-1 molecules *in vivo*. We show that YB-1 plays a critical role in early development in mice. The targeted disruptions were fatal in the late embryonic stage, and

*This work was supported by a grant-in-aid for scientific research on the priority area of ABC proteins, Core Research for Evolutional Science and Technology (CREST) of the Japan Science and Technology Corp. (JST), the second-term comprehensive 10-year strategy for cancer control from the Ministry of Health and Welfare of Japan, and the Cancer Research fund from Ministry of Education, Culture, Sports, Science, and Technology, Japan. The costs of publication of this article were defrayed in part by the payment of page charges. This article must therefore be hereby marked "*advertisement*" in accordance with 18 U.S.C. Section 1734 solely to indicate this fact.

[S] The on-line version of this article (available at http://www.jbc.org) contains supplemental Experimental Procedures and Figs. S1 and S2.

[1] To whom correspondence should be addressed. Tel.: 81-93-691-7423; Fax: 81-93-692-6233; E-mail: uchiumi@med.uoeh-u.ac.jp.

[2] The abbreviations used are: PCNA, proliferating cell nuclear antigen; MEF, mouse embryonic fibroblasts; PBS, phosphate-buffered saline; siRNA, small interfering RNA; FITC, fluorescein isothiocyanate; PI3K, phosphatidylinositol 3-kinase; NTD, neural tube defect; E, embryonic day; S6K, p70 S6K.

TABLE 1

YB-1 deficiency causes embryonic lethality

Embryos at the indicated stages were isolated from intercrosses of heterozygous animals, and the total numbers (n) of intact as well as disintegrated or resorbed embryos were counted. For calculation of % expected (−/−): $n(-/-) \times 100 \times 3/n(+/+) + n(+/-)$.

Stage	Litters	Embryos	+/+	+/−	−/−	Abnormal (−/−)	% expected (−/−)
E10.5	15	120	27	59	34	2	118
E11.5	13	66	17	33	16	9	96
E12.5	14	82	18	48	16	16	73
E13.5	18	120	36	50	34	34	118
E14.5	12	81	18	50	13	13	57
E15.5	7	56	18	25	11	11	77
E16.5	3	17	5	9	3	3	64
E17.5	9	55	26	25	3	3	18
E18.5	3	28	5	20	1	1	12
Adult	33	185	67	118	0		0

animals showed defects in the anterior neural tube. Furthermore, we investigated the role of YB-1 in cell proliferation and the transformation activity of MEFs.

EXPERIMENTAL PROCEDURES

Animals—Animals were mated overnight, and the females were examined for a vaginal plug the following morning. Noon on the day of vaginal plug detection was recorded as day E0.5. All animal experiments were carried out according to the guidelines for animal experimentation at Kyushu University, Japan, and the University of Occupational Environmental Health, Japan. All experimental protocols were approved by the ethics committee of Kyushu University and the University of Occupational Environmental Health, Japan.

In Situ Hybridization—*In situ* hybridization of digoxygenin-labeled probes was performed as described previously (18). The digoxigenin-labeled hybridization probe was prepared from an *in vitro* transcription system (Promega, Madison, WI) using the mouse YB-1 full-length cDNA (11).

Generation of YB-1 (MSY-1)-deficient Mice—Embryonic stem cells were transfected with the linearized targeting construct that deleted exons 5 and 6 of mouse *YB-1* (*MSY-1*) (17), and recombinant clones were selected and microinjected into C57BL/6 mouse blastocytes. Chimeric males that transmitted the mutant allele to the germ line were mated with C57BL/6 females, and germ line transmission of the mutant allele was confirmed by Southern blot analysis (17). Heterozygous offspring were intercrossed to produce homozygous mutant animals. For embryo genotyping, DNA was extracted from the corresponding embryonic tissue removed from microscope sections and amplified by 30 cycles of PCR at 94 °C for 30 s, 58 °C for 30 s, and 68 °C for 1 min using the following primers: YB5-1, 5′-GGAAACCATGTGGAGATGTC, and YB3-1, 5′-GGAGGTTCAAAAGCACACTC (wild-type allele); neo5, 5′-GATTGCACGCAGGTTCTCCG, and neo3, 5′-CAAGAAGGCGATAGAAGGCG (mutant allele).

Immunohistochemistry—Cells seeded the previous day on glass coverslips were washed with phosphate-buffered saline (PBS), fixed with 3.7% formaldehyde for 30 min, rinsed twice with PBS, and then incubated with PBS containing 0.1% Triton X-100 (Sigma) for 30 min. Next, the coverslips were washed with PBS, incubated with 10% goat serum for 1 h at room temperature in a humidified container, and then incubated for 1 h with FITC-conjugated phalloidin (Sigma). After washing three times with PBS, glass slides were mounted using Slowfade mounting medium (Molecular Probes). FITC-conjugated phalloidin (Sigma) was diluted 1:200 and used to detect F-actin organization in mouse tissue and MEF cells.

Immunoblot Analysis—Embryos (E11.5) and MEF cells were lysed with radioimmunoprecipitation (RIPA) buffer (50 mM Tris-HCl, pH 7.5, 1 mM EDTA, 150 mM NaCl, 0.1% SDS, 0.5% sodium deoxycholate, and 1% Nonidet P-40) and subjected to immunoblot analysis as described previously (17) using polyclonal antibodies against YB-1 (19) and monoclonal antibodies against β-actin (AC-15; Sigma), EF-1 (Upstate, Charlottesville, VA), p70 S6K (BD Biosciences), eIF4E (BD Biosciences), Akt (9272; Cell Signaling, Danvers, MA), and PCNA (sc-56, Santa Cruz Biotechnology, Santa Cruz, CA). Band intensities were measured by Image Gauge (Fujifilm, Tokyo, Japan).

Immunohistochemical Analysis of Mouse Embryo Sections—Mouse embryo tissue was fixed with 10% buffered formalin and embedded in paraffin. Sagittal sections (5 μm thick) were cut and mounted on silane-coated glass slides. After routine deparaffination and rehydration through gradient ethanol immersions, the slides were steam-heated for 20 min to expose the antigen. Endogenous peroxidase activity was quenched using 3% (v/v) H_2O_2 followed by three 5-min washes in PBS containing 0.2% (v/v) Triton X-100, and the sections were blocked with 10% (v/v) normal goat serum in PBS. Specimens were incubated for 1 h with the YB-1 and β-actin antibody diluted in PBS containing 0.3% (v/v) Triton X-100 and 0.1% (w/v) bovine serum albumin, followed by three 5-min washes in PBS, and then incubation with the FITC-conjugated goat anti-rabbit antibody (Kirkegaard & Perry Laboratories, Gaithersburg, MD) for 30 min. Specimens were counterstained with hematoxylin for 30 s and washed with tap water. The sections were immediately dehydrated by sequential immersion in gradient ethanol and xylene, then mounted with Permount (ProSciTech, Australia), and coverslips. Images were obtained using a Leica DMRX upright microscope coupled with a digital camera (Leica, Germany).

Culture of Mouse Embryonic Fibroblasts (MEF)—Heterozygous male and female mutant mice were bred to obtain wild-type (*YB-1*$^{+/+}$), heterozygous (*YB-1*$^{+/-}$), and homozygous mutant (*YB-1*$^{-/-}$) embryos. Mouse embryonic fibroblasts were cultured in Dulbecco's modified Eagle's medium with 10% fetal bovine serum. Outgrowths were inspected daily, and their development was monitored by photography.

Proliferation Assay—Cells (1×10^4) were seeded in triplicate in 35-mm dishes and grown under high serum (10% fetal bovine

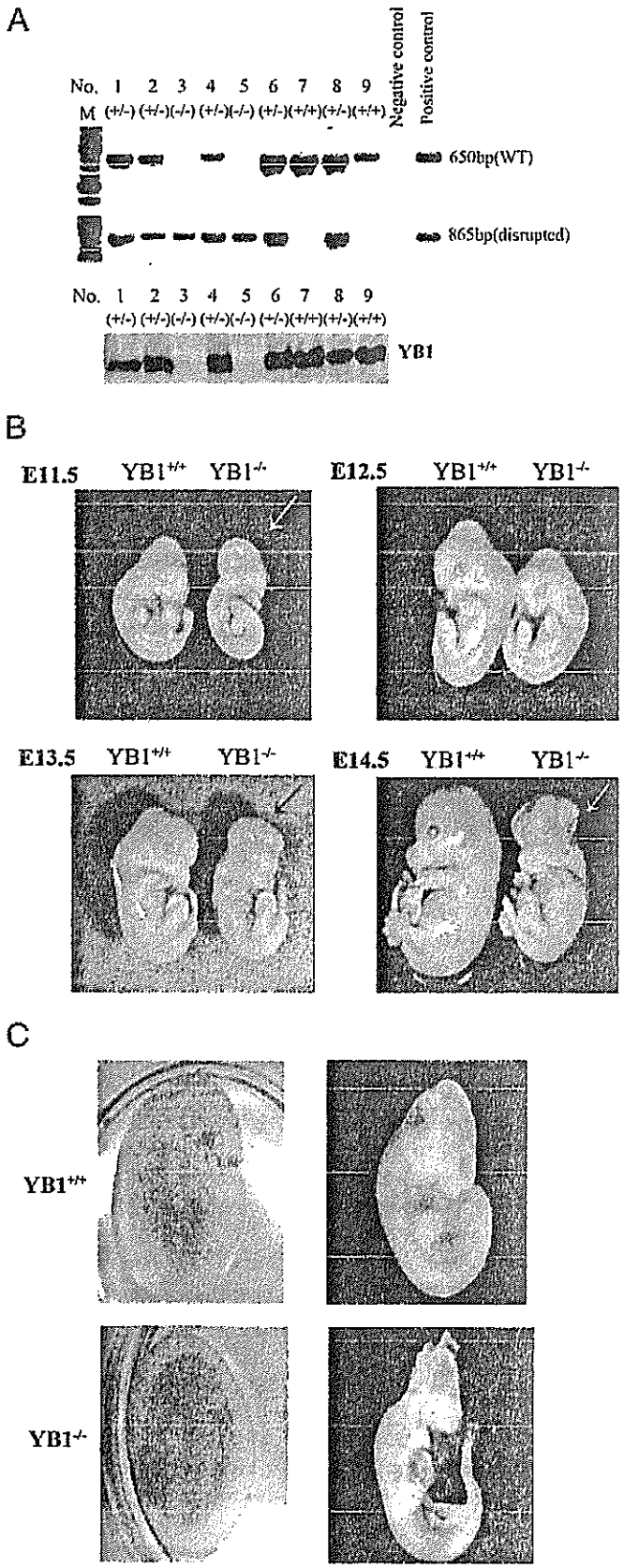

FIGURE 1. **Exencephaly in *YB-1*$^{-/-}$ embryos.** *A*, PCR genotyping of yolk sac DNA from nine E11.5 embryos. *M*, size marker. Bands of 650 bp of wild-type (*WT*) and 865 bp of mutant (*disrupted*) are shown. Total embryo protein (E11.5) was isolated, and the amount of YB-1 protein was determined by Western blotting using a polyclonal YB-1 antibody (*lower panel*). *B*, *YB-1*$^{+/+}$ and *YB-1*$^{-/-}$ embryos at E11.5 to E14.5 stages of development. Exencephaly was observed in various embryonic stages of YB-1 null mice. *Arrow* indicates brain tissue outside of the calvarium in exencephalic embryos. *C*, *YB-1*$^{+/+}$ and *YB-1*$^{-/-}$ embryos at E10.5 stage of development. *YB-1*$^{-/-}$ embryos show severe hemorrhage (*bottom left panel*) and anemia (*bottom right panel*) in comparison with wild-type embryos (*top panels*).

serum) conditions. Dishes were trypsinized and counted daily using a Coulter-type cell size analyzer (CDA-500, Sysmex, Kobe, Japan).

Transformation Assay—Cells (3×10^3) were seeded in triplicate in 10-cm dishes and maintained in Dulbecco's modified Eagle's medium supplemented with 10% fetal bovine serum and antibiotic-antimycotic (Invitrogen). Growth medium was changed every 3 days. After 14–16 days, transformation efficiency was evaluated by counting individual foci. All transformation assays were repeated at least three times. Representative plates were stained with Giemsa and photographed.

Anchorage-independent Growth—Growth in soft agar was assayed in 35-mm dishes prepared with a lower layer of 0.7% agar (Invitrogen) overlaid with top agar (0.4%) containing 5×10^3 suspended cells. Cells were fed every 3 days with media. Fifteen days after plating, colonies were stained with 2% crystal violet, and colonies with >50 cells were counted on an inverted microscope (Olympus, Tokyo, Japan).

Knockdown Analysis Using siRNA—siRNA transfections were performed according to the manufacturer's instructions (Invitrogen). Briefly, cells cultured in 35-mm dishes were transfected with stealth RNA interference-negative control duplexes and YB-1 siRNA oligonucleotides (CAACGUCGGUAUCGCCGAAACUUCA) at a final concentration of 100 μM using Lipofectamine 2000 (Invitrogen). After transfection, cell number and cell volume were quantified using an electronic sizing technique with a CDA-500 Coulter-type cell size analyzer (Sysmex). Cells were also harvested for Western blotting (17).

RESULTS

Disruption of YB-1 Causes Embryonic Lethality—To elucidate the function of YB-1 during mouse development, we used gene targeting to generate YB-1-deficient mice. Although the heterozygous offspring appeared normal and fertile (Table 1), Southern blot analysis of tail DNA from 3-week-old mice revealed that no live animals (of 144 births from heterozygote crosses) were homozygous for the *YB-1* mutation. Thus, loss of YB-1 results in embryonic lethality.

To determine the time at which the *YB-1* mutant becomes lethal, we examined embryos from *YB-1*$^{+/-}$ intercrosses at various developmental stages. PCR genotyping data of nine mouse embryos at E11.5 revealed two wild-types, five heterozygotes, and two homozygous mutants, in accordance with the expected Mendelian ratio (Fig. 1*A* and confirmed by PCR with four additional primer sets; data not shown). In contrast to wild-type embryos, the growth of *YB-1*$^{-/-}$ embryos appeared retarded as early as E10.5 (Fig. 1*B*). Most *YB-1*$^{-/-}$ embryos had been resorbed by E17.5 and *YB-1*$^{-/-}$ embryos died between E14.5 and E18.5 (Table 1). The phenotype of *YB-1*$^{-/-}$ embryos includes retarded growth, hemorrhage, and severe anemia but is otherwise normal in appearance (Fig. 1*C*).

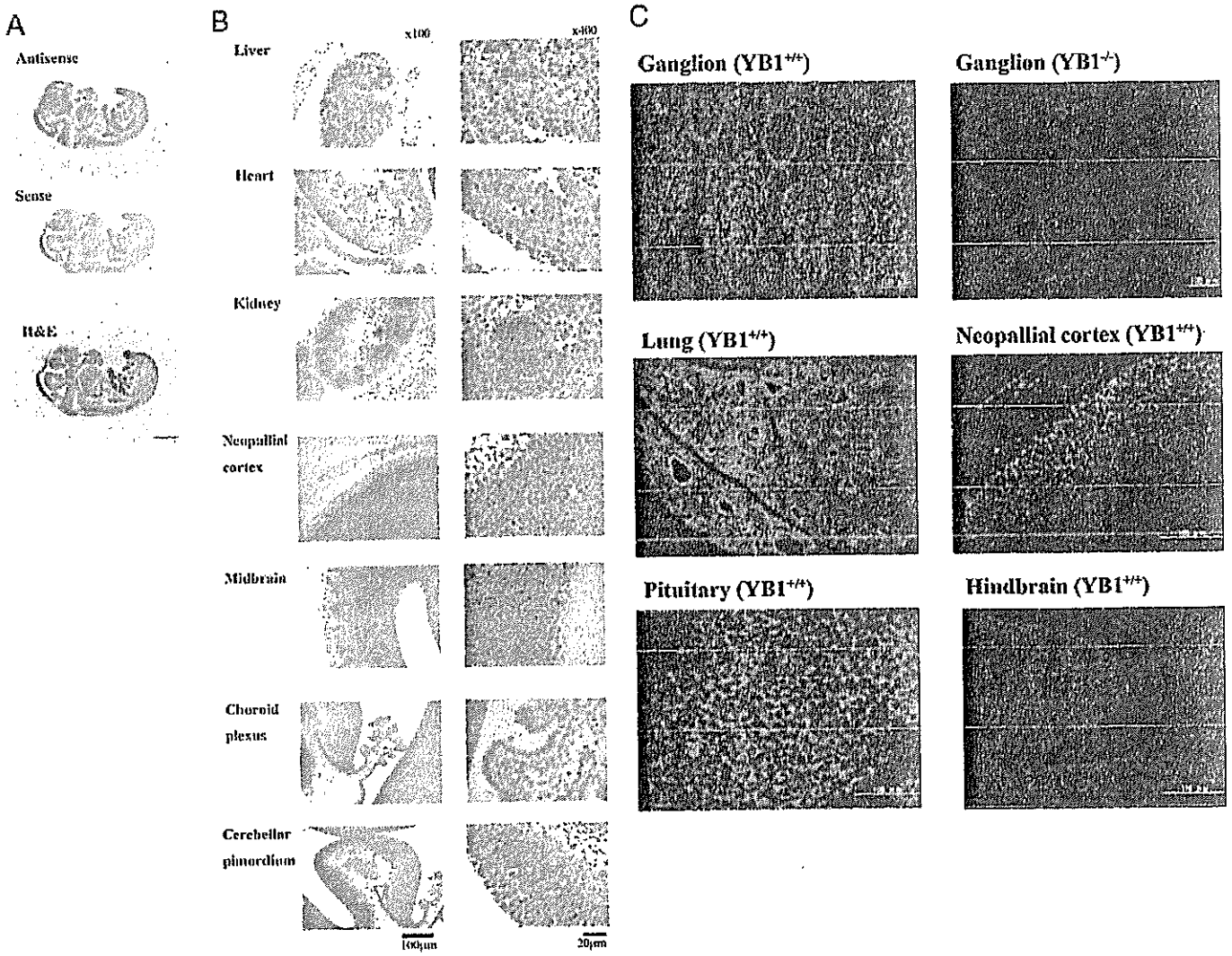

FIGURE 2. **YB-1 expression in embryonic tissues.** *A*, nonradioactive *in situ* hybridization of wild-type E13.5 mouse embryos with antisense or sense YB-1-specific probes shows that YB-1 is expressed in the whole embryo region. *Sense*, negative control; *H&E*, hematoxylin and eosin staining. *Scale bar* = 2 mm. *B*, *in situ* hybridization of wild-type E13.5 embryos showing expression of YB-1 in mouse organs. *Left panel*, *scale bar* = 100 μm. *Right panel*, *scale bar* = 20 μm. *C*, immunohistochemistry showing YB-1 expression in wild-type and YB-1 null E13.5 embryos. No staining was observed in the ganglion of the *YB-1*$^{-/-}$ mouse. *Scale bar* = 100 μm.

Mouse YB-1 Is Expressed in Most Tissues during Embryogenesis—We reported previously that human YB-1 is expressed ubiquitously in the adult (19). The YB-1 transcript and protein have also been detected in mouse embryonic stem cells (17). To determine whether the expression of mouse YB-1 is developmentally regulated, we performed *in situ* hybridization on mouse embryos tissue sections at E13.5. We found that mouse *YB-1* mRNA is expressed at whole body, specifically at high levels in the brain region (Fig. 2, *A* and *B*). Expression in the brain is widespread, with some enrichment in the cortical plate, diencephalons (thalamus), roof of the neopallial cortex, and choroid plexus extending into lateral ventricle, midbrain, and cerebellar primordium (Fig. 2*B*). *YB-1* mRNA is also strongly expressed in the posterior mesoderm, the craniofacial region, root ganglion, kidney, liver, head mesoderm, and in the developing heart (Fig. 2*B*). These data support a critical role for *YB-1* expression during embryonic development.

YB-1 protein expression in E13.5 embryos is almost ubiquitous, with high expression detected in the central nervous system, lung, kidney, and heart (Fig. 2*C*). YB-1 was predominantly localized to the cytoplasm region in wild-type embryos. No expression was detected in either connective tissues or bone of wild-type embryos and was absent from *YB-1*$^{-/-}$ embryos (Fig. 2*C*).

Neural Tube Closure Is Impaired in YB-1-deficient Mice—As shown in Fig. 1*B*, *YB-1*$^{-/-}$ embryos were smaller than their wild-type littermates, although no gross abnormalities were observed in organ or limb development. When examined at E10.5 to E13.5, ~30% of the *YB-1*$^{-/-}$ embryos exhibited exencephaly in the forebrain, midbrain, and hindbrain regions (12/80 *YB-1*$^{-/-}$ embryos) (Fig. 1*B*). Almost all of the mutant embryos were pale and anemic, as a consequence of severe blood loss through hemorrhage (seen as petechial and paintbrush patterns in Fig. 1*C*).

Histological analysis of other parts of the mutant embryos revealed that the *YB-1* mutation does not affect organogenesis, because all major organs were intact (data not shown). Exencephaly typically reflects a defect in closure of the anterior neu-

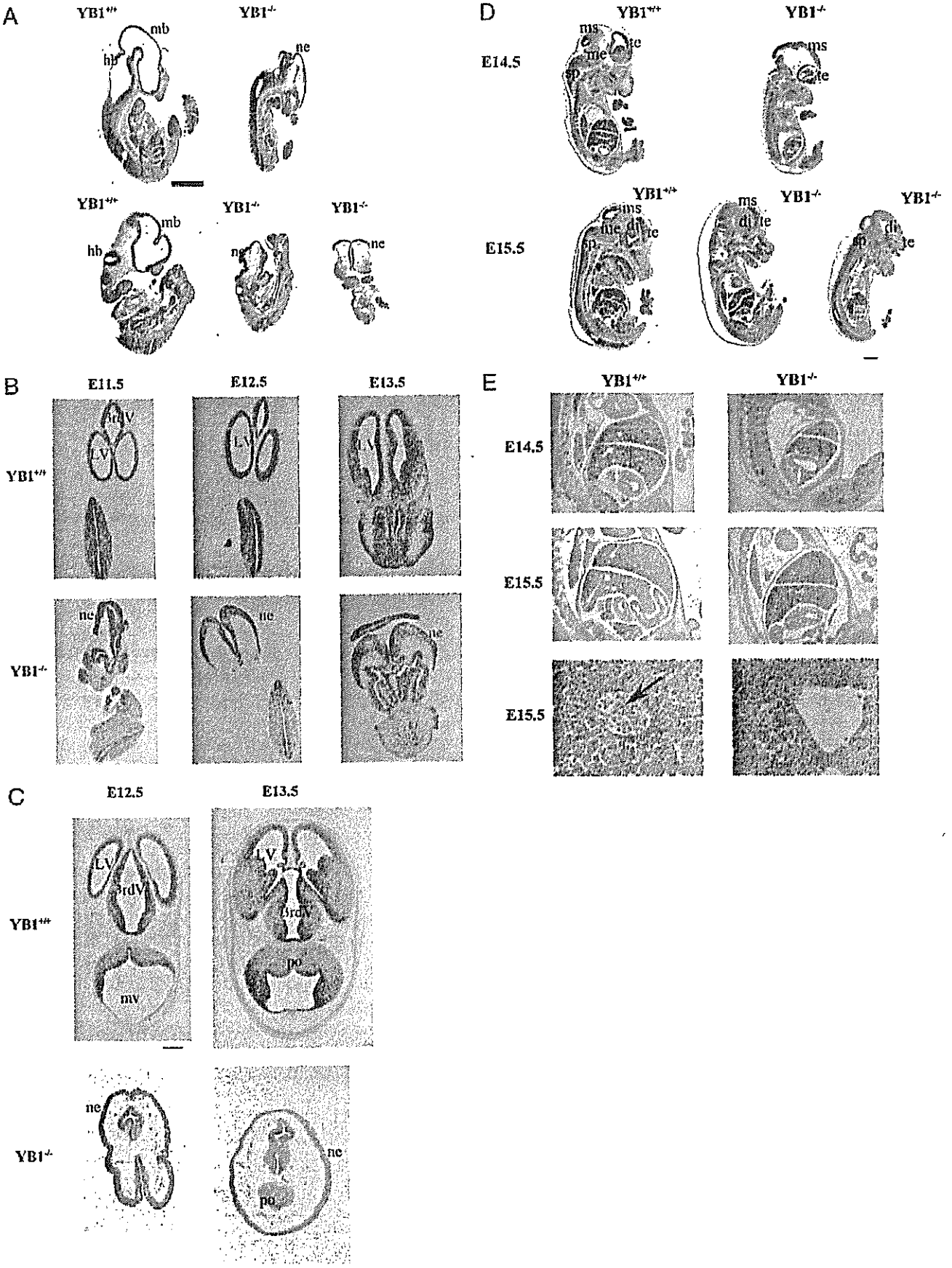

ral tube, which normally occurs between E8.5 and E9.5 (20). Fig. 3 showed a severe brain malformation characterized by exencephaly, expanded midbrain, and a disrupted cortical zone. Examination of older embryos (E13.5 to E15.5) revealed that the mutant brains failed to develop further.

Frontal and cross-sections of the hindbrain region of the E11.5 to E13.5 neural tube defect (NTD) embryos clearly demonstrate incomplete neural tube closure (Fig. 3, *B* and *C*), and the anterior neural tubes of most E10.5 to E11.5 *YB-1*$^{-/-}$ embryos failed to close with varying degrees of severity. No other cranial or neural tube abnormalities such as holoprosencephaly or impaired caudal neural closure were observed. Those *YB-1*$^{-/-}$ mice that achieved skull closure also possessed major brain structures but demonstrated retarded development of the maxilla and mandible (Fig. 3*D*). Most E15.5 *YB-1*$^{-/-}$ embryos had a subcutaneous edema of the whole body (Fig. 3*D*), which was not observed in wild-type and heterozygous mice. Moreover, fetal livers of *YB-1*$^{-/-}$ embryos were smaller than those of their *YB-1*$^{+/-}$ and *YB-1*$^{+/+}$ littermates, which is suggestive of hepatic hematopoiesis (Fig. 3*E*). *YB-1*$^{-/-}$ embryos were also anemic as a result of macroscopically detectable defects in erythropoiesis of the fetal livers (Fig. 3*E*). These data suggest that exencephaly, smaller size of organ, and severe hemorrhage account for the embryonic lethality of the *YB-1* mutation.

Enhanced EF-1 Expression in YB-1$^{-/-}$ *Embryos*—Using whole-cell extracts of eight E11.5 mouse embryos (YB-1$^{+/+}$ ($n = 1$), YB-1$^{+/-}$ ($n = 5$), and YB-1$^{-/-}$ ($n = 2$)), the expression of other proteins involved in the regulation of translation was examined by immunoblotting. Western blotting using antibodies against the YB-1 N- and C-terminal ends revealed that E11.5 *YB-1*$^{-/-}$ embryos did not express either the full-length or the truncated YB-1 protein (Fig. 4*A*; data not shown). *YB-1*$^{+/-}$ embryos expressed ~70–80% as much YB-1 as wild-type embryos. The expression of the serine/threonine protein kinase p70 S6K (S6K) was slightly reduced in *YB-1* null embryos compared with wild-type and heterozygous embryos, whereas human eukaryotic translation initiation factor 4E (eIF4E), Akt, and PCNA expression was unchanged. However, translational elongation factor-1 (EF-1) was overexpressed in *YB-1*$^{-/-}$ embryos, which might reflect a compensatory mechanism.

Decreased Proliferation in YB-1$^{-/-}$ *MEFs*—To examine the molecular basis of YB-1 in cellular proliferation, we established MEFs from wild-type ($n = 4$), *YB-1*$^{+/-}$ ($n = 4$), and *YB-1*$^{-/-}$ ($n = 4$) embryos from three independent litters at E13.5. Heterozygous MEFs (numbers 2, 56, 72, and 73) expressed approximately half as much YB-1 as wild-type MEFs, whereas *YB-1* null MEFs (numbers 3, 60, 74, and 75) expressed no YB-1. PCNA expression was comparable between all MEFs (Fig. 4*B*). During the first three passages, cell proliferation and population doubling was comparable between *YB-1*$^{+/+}$, *YB-1*$^{+/-}$, and *YB-1*$^{-/-}$ MEFs. From passages 4 to 5 onward, all *YB-1*$^{-/-}$ MEFs analyzed showed greatly reduced proliferation and a reduction in cell numbers under base-line culture conditions (Fig. 4*C*). *YB-1*$^{+/-}$ and *YB-1*$^{+/+}$ MEFs proliferated at a similar rate. *YB-1*$^{-/-}$ MEFs exhibited premature senescence and an extended crisis as determined by an enlarged and flattened cell morphology (Fig. 5*B*). After 100 days of culture, *YB-1*$^{-/-}$ MEF cells showed reduced cell proliferation and density, which could be completely recovered to wild-type levels by expression of the YB-1 vector (Fig. 4*D*). YB-1 expression from this vector was confirmed by Western blotting (Fig. 4*B*). These data demonstrate the importance of YB-1 in cell proliferation and maintaining cell morphology.

NTD and Actin Assembly—NTDs involving mutations in genes that regulate actin arrangement at the cell membrane or play alternative roles in actin synthesis have been reported previously (21). In all cases, the defects included exencephaly caused by a failure of cranial neural fold elevation, as observed in the *YB-1*$^{-/-}$ embryos. In addition, YB-1 has been shown to associate with β-actin mRNA and the actin protein (11, 22). We used immunofluorescence to investigate whether β-actin synthesis and rearrangement are affected in E13.5 *YB-1*$^{-/-}$ embryos, and we showed that β-actin protein levels were greatly reduced in the cephalic region of the *YB-1* null embryo, in comparison with the wild type (Fig. 5*A*).

Phalloidin staining of E13.5 brain sections revealed a substantially decreased accumulation of F-actin along the basal edge of neuroepithelial cells in the null mutant embryo compared with the wild type (Fig. 5*B*). These data suggest that the reduced β-actin levels and F-actin filament formation might be responsible for the NTDs of *YB-1*$^{-/-}$ embryos. In some mutant animals, a reduced apical constriction of the neuroepithelial cells within this region was also observed.

We next examined the role of YB-1 in cell morphology and organization of the actin cytoskeleton. Wild-type MEFs had an elongated morphology and an F-actin-rich polarized cytoskeleton. In contrast, *YB-1*$^{-/-}$ MEFs were round in shape, with lower cell density (Fig. 5*B*). Most strikingly, mutant cells lacked appreciable F-actin structures such as fibers or bundles. Instead, a small amount of F-actin was seen as a fuzzy phalloidin signal that was consistently found in the subcellular region rather than in the cell perimeter (Fig. 5*B*). These results show that YB-1 is essential for organizing F-actin and maintaining the cell shape of MEFs.

As YB-1 possesses RNA binding activity and has been shown to regulate protein synthesis and mRNA stability (11, 23), we next investigated the interaction of YB-1 with β-actin mRNA.

FIGURE 3. **Neural tube defects in YB-1 mutant mice.** *A*, histological profile of sagittal sections at E10.5 showing exencephaly and defective development of cephalic area in mutant embryos. *hb*, hindbrain; *mb*, midbrain; *ne*, neuroepithelium. *Scale bar* = 1 mm. *B*, histological profile of whole E11.5–13.5 embryo frontal sections stained with hematoxylin and eosin staining showing severe disturbance of cephalic area in exencephalic embryos. YB-1$^{-/-}$ mutants exhibit open neural tubes. *Scale bar* = 200 μm. *C*, cross-sections of wild-type and *YB-1*$^{-/-}$ E12.5 to E13.5 mouse embryos showing defective neural tube closure. *YB-1*$^{-/-}$ mouse embryos were surrounded by the everted neuroectoderm of the midbrain and hindbrain. *3rdV*, third ventricle; *LV*, lateral ventricle; *mv*, mesencephalic vesicle; *po*, pons. *Scale bar* = 1 mm. *D*, sagittal sections of wild-type and *YB-1*$^{-/-}$ E14.5 to E15.5 mouse embryos showing defective neural tube closure and exencephalic phenotype of the mutant embryo (*upper right panel*). Some *YB-1*$^{-/-}$ embryos (*bottom center panels*) exhibit anterior brain structure, skull closure, and size comparable with wild-type littermates. *ms*, mesencephalon; *me*, medulla; *te*, telencephalon; *di*, diencephalon; *sp*, spinal cord. *Scale bar* = 1 mm. *E*, sagittal sections of wild-type and *YB-1*$^{-/-}$ E14.5 to E15.5 mouse embryos showing smaller liver size of the mutant embryo (*right panel*). Erythrocytes (*arrow*) are present in YB-1$^{+/+}$ liver region, but not in YB-1$^{-/-}$ liver (*lower panel*).

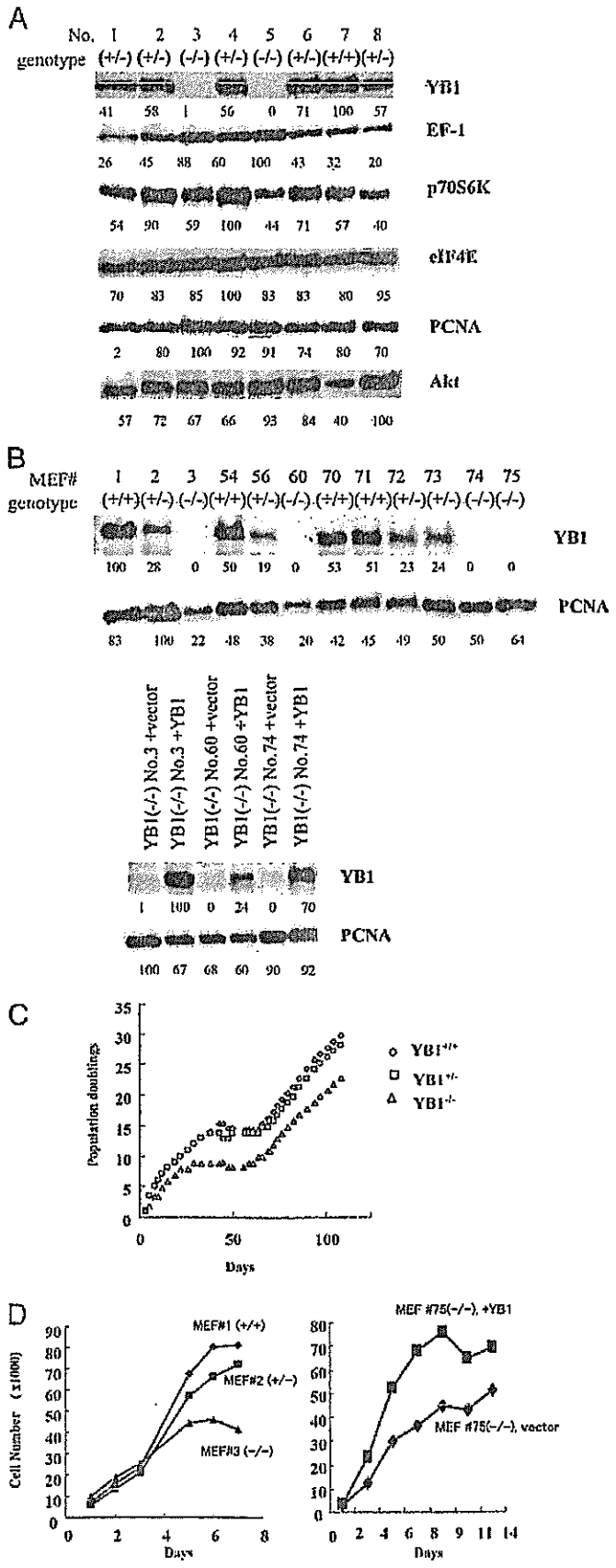

FIGURE 4. **Elevated EF-1 expression in *YB-1*$^{-/-}$ embryos and decreased growth of *YB-1*$^{-/-}$ MEFs.** *A*, Western blot analysis of protein expression in E11.5 embryonic mouse tissues. Total protein derived from eight PCR-genotyped mouse embryo tissues (50 μg of protein per lane) was immunoblotted using a specific antibody against YB-1, EF-1, p70 S6K, eIF4E, Akt, and PCNA. Elevated levels of EF-1 were observed in *YB-1*$^{-/-}$ MEFs (*lanes 3* and *5*). Relative band intensity (%) is presented. *B*, establishment of MEFs. Western blot analysis of YB-1 and PCNA expression levels after establishment of immortalized, PCR-genotyped MEF clones (*left panel*) and immortalized YB-1 null MEF clones transfected with a pIRES (control) vector or pIRES-YB-1 plasmid (*right panel*). *C*, growth curves of *YB-1*$^{+/+}$, *YB-1*$^{+/-}$, and *YB-1*$^{-/-}$ MEFs. One representative experiment is shown. Population doubling curves were determined using trypan blue exclusion. *D*, proliferation rate of MEFs as assessed by cell counts. *YB-1*$^{+/+}$ (*diamonds*), *YB-1*$^{+/-}$ (*squares*), and *YB-1*$^{-/-}$ (*triangles*) were inoculated at 5×10^4 cells/ml. The cell numbers were determined at the time points indicated. Ectopic expression of wild-type YB-1 reversed the proliferation defect (*right panel*).

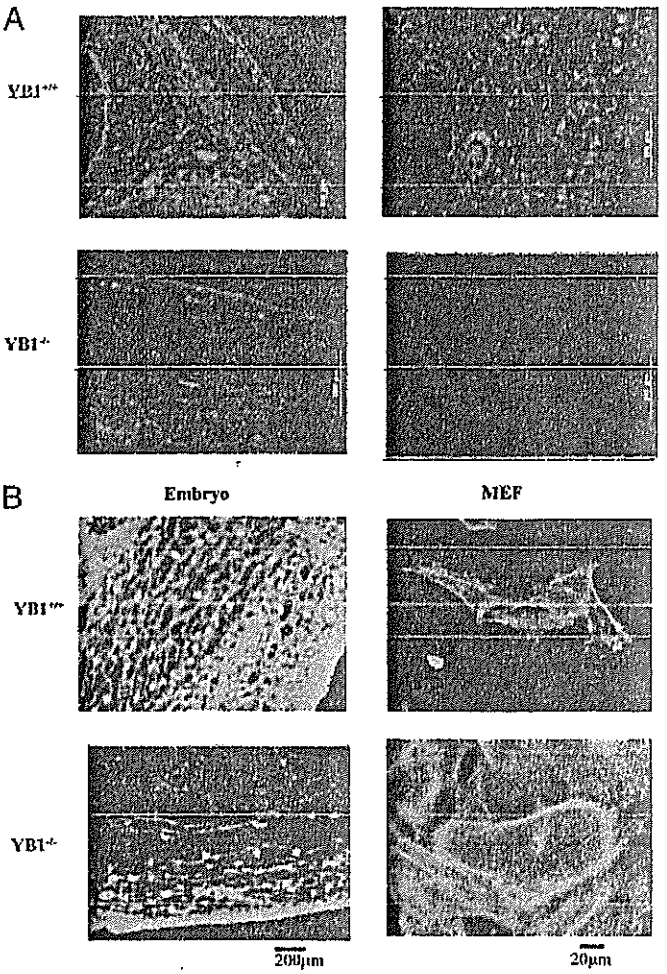

FIGURE 5. **Actin expression in the brain of wild-type and mutant embryos.** *A*, at low magnification, β-actin was shown to be ubiquitously expressed in wild-type embryos; however, *YB-1*$^{-/-}$ embryos demonstrated local reduction and derangement of β-actin expression. This is especially obvious in connective tissue-filled central nervous system supportive tissues. *B*, immunohistochemistry with FITC-phalloidin was performed in E10.5 mouse embryos (*top panels*) and MEFs (*bottom panels*). Mutant embryos showed reduced F-actin structures. Normal cytoskeletal structures can be seen in wild-type MEFs. Stress fiber formation was reduced in *YB-1*$^{-/-}$ MEFs, and cells were flatter and larger than wild-type MEFs.

An *in vitro* RNA gel shift assay was performed using purified recombinant YB-1 and a probe corresponding to full-length β-actin mRNA. Recombinant YB-1 clearly bound to β-actin mRNA, whereas the control glutathione *S*-transferase protein failed to do so (supplemental Fig. 1*A*). To determine whether the interaction occurs *in vivo*, we performed reverse transcrip-

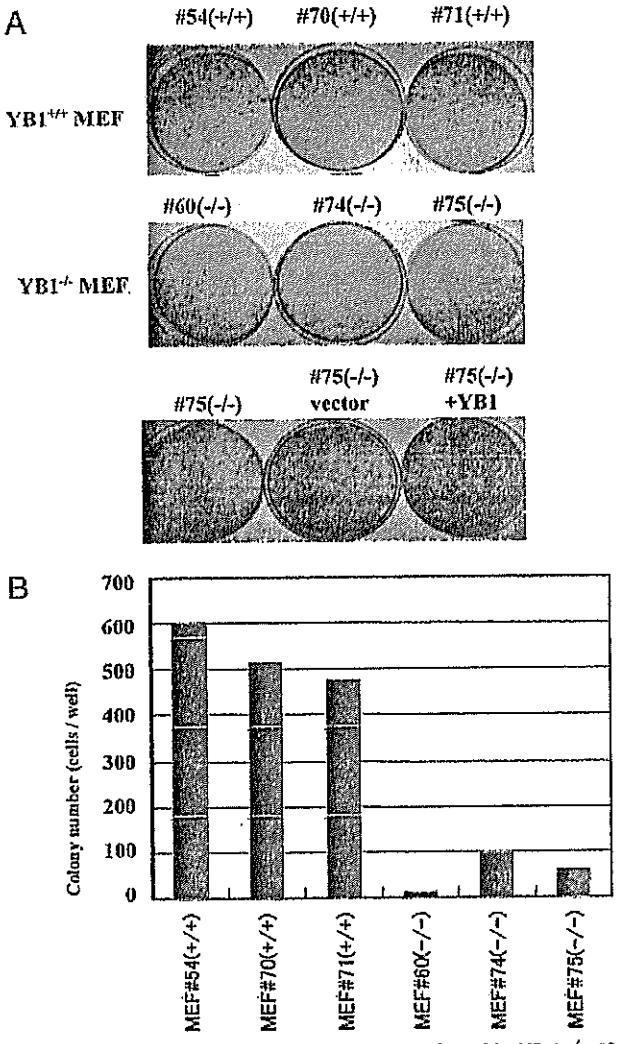

FIGURE 6. **Colony transformation activity was reduced in *YB-1*$^{-/-}$ MEFs but could be rescued by re-expression of YB-1.** *A*, three *YB-1*$^{-/-}$ MEF cell lines (*middle panel*) demonstrated reduced transformation activity compared with wild-type MEFs (*top panel*), following 2% Giemsa staining. Introduction of recombinant YB-1 restored the transformation activity (*bottom panel*). *B*, three *YB-1*$^{-/-}$ MEF cell lines demonstrated reduced colony forming activity compared with wild-type MEFs, following 2% crystal violet staining. Cells were assayed in triplicate.

tion-PCR using β-actin-specific primers on mRNA isolated by co-immunoprecipitation with YB-1. β-Actin transcript was amplified from wild-type but not from *YB-1*$^{-/-}$ MEFs (supplemental Fig. 1*B*), suggesting that YB-1 indeed interacts with β-actin mRNA in MEFs. This interaction might regulate the activity or availability of β-actin in protein synthesis.

Reduced Anchorage-independent Growth by YB-1$^{-/-}$ *Cells*—We established three wild-type and three *YB-1*$^{-/-}$ immortalized MEF lines after continuous culturing for more than 6 months to investigate their spontaneous transformation ability *in vitro*. Although the wild-type cells did not show any signs of a decrease in proliferative rate, *YB-1*$^{-/-}$ MEFs failed to undergo morphological transformation and remained contact-inhibited after 2 weeks of cultivation (Fig. 6*A*, *upper* and *middle panel*). Following re-expression of transgenic YB-1, however, the MEFs underwent morphological transformation, whereas vector-only transduced MEFs failed to do so (Fig. 6*A*, *lower panel*). Furthermore, a one-fifth reduction in anchorage-independent growth was observed in the *YB-1*$^{-/-}$ MEF clones (Fig. 6*B*).

To confirm these results, we investigated whether knockdown of endogenous YB-1 via siRNA affected cell growth and size. The siRNA oligonucleotide was directed against the YB-1 C-terminal region, with the exception of the cold-shock domain. Western blot analysis of siRNA-transfected MEFs revealed that YB-1 protein levels were reduced to 20% of wild-type levels 72 h after transfection (Fig. 7*A*). YB-1 siRNA-transfected MEFs also showed a reduced growth rate and were ~10% larger (22 μm in diameter) than the negative control transfected MEFs (20 μm in diameter) (Fig. 7, *B* and *C*). This phenomenon was consistent with our earlier observations of *YB-1*$^{-/-}$ MEFs (Fig. 5*B*) and shows that YB-1 is involved in both regulating cell growth rates and cell size. In an anchorage-independent transformation assay in soft agar, YB-1 expressing MEFs (number 70) showed morphological transformation, but siRNA-transfected MEFs demonstrated reduced transformation activity (Fig. 7*D*). These results confirm our earlier finding that YB-1 is necessary for anchorage-independent transformation activity (see also Fig. 6*A*).

DISCUSSION

This study demonstrates that YB-1 plays a critical role in DNA repair, transcription, mRNA turnover, and translational control. Previously, Lu *et al.* (24) reported that targeted disruption of *YB-1* exon 3 (encoding part of the cold-shock domain) causes embryonic lethality and showed that YB-1 is important for cellular stress responses and prevention of premature senescence after E13.5. In this study, we demonstrated that *YB-1*$^{-/-}$ embryos exhibit severe growth retardation and progressive mortality after E10.5, revealing a nonredundant role for YB-1 in early embryonic development. Our study design disrupted *YB-1* exons 5 and 6, encoding a nonspecific RNA binding region of the protein. Western blot analysis using an antibody against the YB-1 C terminus revealed that the YB-1 protein was completely absent from the E13.5 *YB-1*$^{-/-}$ embryo (Fig. 4*A*).

In this experiment, we first demonstrated that β-actin expression and F-actin formation were reduced in the *YB-1* null embryo and *YB-1*$^{-/-}$ MEF, suggesting that the neural tube defect is caused by abnormal cell morphology and actin assembly within the neuroepithelium. We also showed that *YB-1*$^{-/-}$ MEFs failed to undergo morphological transformation in culture cells and suggested that YB-1 is involved in cell proliferation.

Although only 20% of YB-1 null mutant mice showed exencephaly (Table 1), this is not an unusual finding, as mouse embryos subjected to inactivation of a critical gene via homologous recombination rarely show NTDs with complete penetrance (25). As an NTD phenotype, exencephaly reflects the failure of neural fold elevation in well defined, mechanistically distinct elevation zones (26). The genes mutated in several mouse NTD models that are involved in actin regulation (*Abl/Arg, Marcs, Mena/Profilin1, Mlp, Sprm, Vcl*) support the postulated role for actin in neural fold elevation and suggest that the NTDs are caused by an absence of the morphogenetic force normally provided by the apical redistribution of actin (25). We

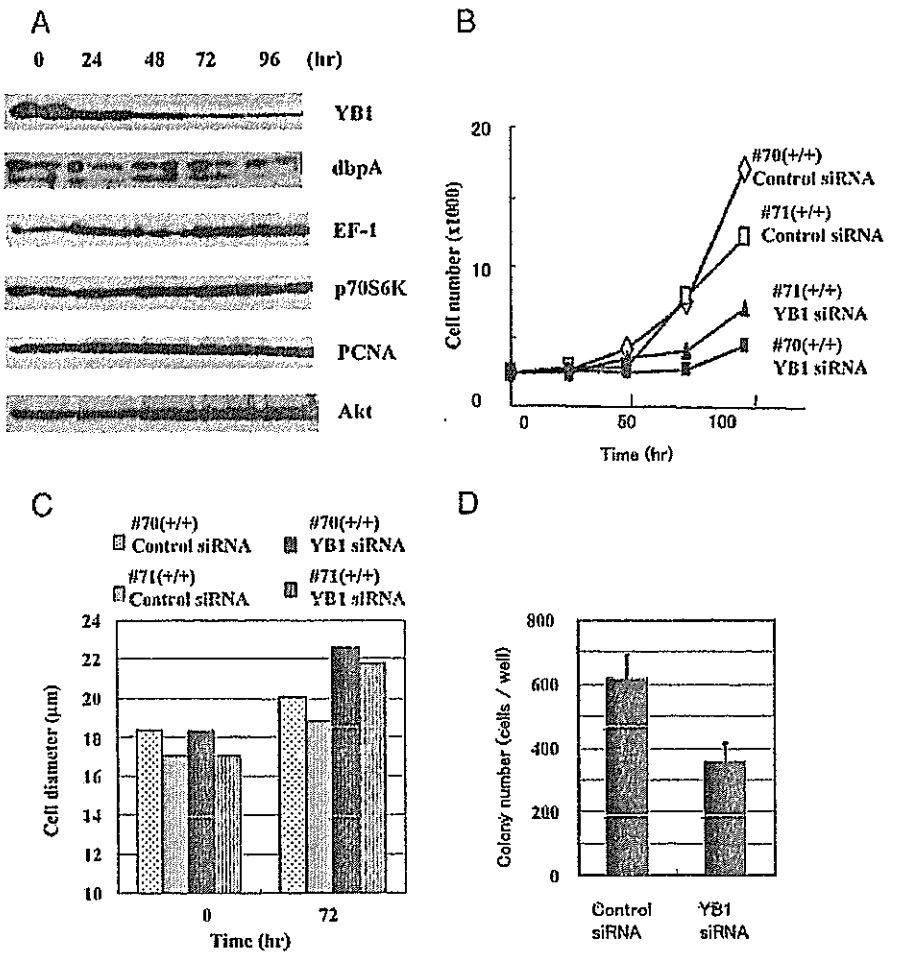

FIGURE 7. **siRNA-mediated YB-1 knockdown in MEFs.** *A*, immunoblot analysis of YB-1 siRNA-transfected MEFs. Wild-type MEFs were transfected with YB-1 siRNA, and total cell lysate (50 μg) was harvested at various time points following transfection and analyzed for indicated protein. Seventy two hours after transfection of siRNA, YB-1 protein levels had reduced by 20%. *B*, proliferation rate of siRNA-mediated MEFs. YB-1 siRNA-transfected cells demonstrated growth retardation compared with wild-type MEFs. *C*, cell size of siRNA mediated MEFs. The cell diameter of transfected MEFs was measured 0 and 72 h after transfection with a Coulter-type cell size analyzer. siRNA-transfected cells demonstrated a larger size (average diameter 22 μm) compared with wild-type cells (average diameter 20 μm). Experiments were performed in triplicate. *D*, siRNA-transfected cells demonstrated reduced colony forming activity compared with wild-type MEFs, following 2% crystal violet staining.

observed that YB-1 impairs translation of the β-actin transcript in a rabbit reticulocyte translation system (data not shown). Similar results have been reported for β-actin (27) and α-globin mRNAs (28). The strong, nonspecific *in vitro* binding of YB-1 to mRNA inhibits translation (29) and is a possible mechanism for regulating actin activity or its availability in protein synthesis. This is consistent with our finding that disruption of YB-1 leads to low β-actin levels and reduced actin assembly (Fig. 5).

Recently, the localization of β-actin mRNA to sites of active actin polymerization has been shown to modulate cell migration and neurite outgrowth (30). This localization requires the oncofetal protein Zipcode-binding protein 1 (ZBP1), which promotes translocation of the β-actin transcript to actin-rich protrusions in primary fibroblasts and neurons. ZBP1 associates with the β-actin transcript in the nucleus and prevents premature translation in the cytoplasm by blocking translation initiation. Interestingly, Matsumoto *et al.* (27) reported an interaction between YB-1 and ZBP1, suggesting that both proteins might coordinate in their regulation of β-actin mRNA localization, protection, and protein synthesis at the correct site. Further elucidation of this interaction should improve the understanding of the molecular mechanisms behind β-actin regulation.

The role of YB-1 in cell proliferation might be executed through its interaction with actin (22), as actin filaments form the contractile ring that cleaves the cell during cytokinesis (31). Alternatively, cell proliferation might be regulated by the effect of YB-1 on the cell cycle proteins cyclin A and cyclin B1, as YB-1 was found to induce strongly elevated levels of cyclin B1 protein in the mitotic stage (32). The targeted disruption of one allele of the chicken Y-box protein gene in DT40 cells results in major defects in the cell cycle (33). In this study, no difference in cyclin A and cyclin B expression was observed in *YB-1*$^{-/-}$ mouse embryos or MEFs (data not shown), suggesting that the expression level of these proteins did not cause the embryonic lethality and abnormality of the *YB-1*$^{-/-}$ mice.

Bergmann *et al.* (34) showed that transgenic mice expressing human hemagglutinin-tagged YB-1 developed diverse breast carcinomas through the induction of genetic instability caused by mitotic failure and centrosome amplification. We observed the spontaneous transformation of wild-type MEFs but showed that *YB-1*$^{-/-}$ MEFs failed to undergo morphological transformation and remained contact-inhibited (Fig. 6*B*). Re-expression of YB-1 restored the transformation activity suggesting that YB-1 is necessary for tumor promotion. Indeed, overexpression of YB-1 mRNA and protein is a hallmark of several human malignant diseases (2, 34), whereas the level of YB-1 protein expression has been linked with the prognosis of breast cancer patients and resistance to chemotherapeutic agents (5).

The nuclear translocation of YB-1 requires phosphorylation by the signal transduction protein Akt (35), which plays a role in tumor formation and progression. Evdokimova *et al.* (36) reported that phosphorylation by Akt also regulates the association of YB-1 with the capped 5′ terminus of mRNA and that activated Akt might relieve translational repression of YB-1-bound mRNA. We investigated the level of Akt protein in wild-type and siRNA-mediated YB-1 knockdown MEFs, but no difference was detected (Figs. 4*A* and 7*A*),

suggesting that YB-1 does not affect Akt protein levels in MEFs.

Target of rapamycin is a downstream kinase in the PI3K/Akt signaling pathway that phosphorylates S6K and translation initiation factor 4E-binding protein (4EBP), thus regulating translation (37). We also observed that S6K protein levels were reduced in YB-1 null mouse embryos, suggesting that YB-1 might be involved in this PI3K signaling pathway. Indeed, YB-1 is transcriptionally down-regulated in PI3K-transformed and Akt-transformed cells (29, 38). YB-1 acts downstream of the target of rapamycin, as the phosphorylation levels of S6K and 4EBP are unchanged in YB-1-overexpressing cells (39). An independent line of evidence has revealed the essential role of protein synthesis in PI3K- and Akt-induced transformation (40).

Activation of eukaryotic elongation factor 1A (eEF-1A) through phosphorylation by S6K (41, 42) enables it to bind to actin and regulate its activity or its availability in protein synthesis (43, 44). eEF-1A mutants have severe defects in cell morphology, the actin cytoskeleton, and actin bundling (44). In mammalian systems, disruption of the actin cytoskeleton results in reduced translation. In this study, we observed that YB-1 co-precipitated with eEF-1A (supplemental Fig. S2), suggesting that eEF-1A might compensate for the function of YB-1 in *YB-1*$^{-/-}$ embryos and MEFs. We also observed that another translational regulatory protein, EF-1, was overexpressed in *YB-1*$^{-/-}$ E11.5 embryos and siRNA-mediated YB-1 knockdown MEFs (Fig. 4*A* and 7*A*), indicative of an alternative compensatory mechanism.

In conclusion, we have described the function of YB-1 in the mouse embryo and in MEFs. We show that it is involved in mouse embryo development, neural tube defects, and cell proliferation.

REFERENCES

1. Makino, Y., Ohga, T., Toh, S., Koike, K., Okumura, K., Wada, M., Kuwano, M., and Kohno, K. (1996) *Nucleic Acids Res.* **24**, 1873–1878
2. Kohno, K., Izumi, H., Uchiumi, T., Ashizuka, M., and Kuwano, M. (2003) *BioEssays* **25**, 691–698
3. Didier, D. K., Schiffenbauer, J., Woulfe, S. L., Zacheis, M., and Schwartz, B. D. (1988) *Proc. Natl. Acad. Sci. U. S. A.* **85**, 7322–7326
4. Ladomery, M., and Sommerville, J. (1995) *BioEssays* **17**, 9–11
5. Kohno, K., Uchiumi, T., Niina, I., Wakasugi, T., Igarashi, T., Momii, Y., Yoshida, T., Matsuo, K., Miyamoto, N., and Izumi, H. (2005) *Eur. J. Cancer* **41**, 2577–2586
6. Asakuno, K., Kohno, K., Uchiumi, T., Kubo, T., Sato, S., Isono, M., and Kuwano, M. (1994) *Biochem. Biophys. Res. Commun.* **199**, 1428–1435
7. Ohga, T., Uchiumi, T., Makino, Y., Koike, K., Wada, M., Kuwano, M., and Kohno, K. (1998) *J. Biol. Chem.* **273**, 5997–6000
8. Swamynathan, S. K., Nambiar, A., and Guntaka, R. V. (1998) *FASEB J.* **12**, 515–522
9. Sommerville, J. (1999) *BioEssays* **21**, 319–325
10. Ashizuka, M., Fukuda, T., Nakamura, T., Shirasuna, K., Iwai, K., Izumi, H., Kohno, K., Kuwano, M., and Uchiumi, T. (2002) *Mol. Cell. Biol.* **22**, 6375–6383
11. Fukuda, T., Ashizuka, M., Nakamura, T., Shibahara, K., Maeda, K., Izumi, H., Kohno, K., Kuwano, M., and Uchiumi, T. (2004) *Nucleic Acids Res.* **32**, 611–622
12. Koike, K., Uchiumi, T., Ohga, T., Toh, S., Wada, M., Kohno, K., and Kuwano, M. (1997) *FEBS Lett.* **417**, 390–394
13. Okamoto, T., Izumi, H., Imamura, T., Takano, H., Ise, T., Uchiumi, T., Kuwano, M., and Kohno, K. (2000) *Oncogene* **19**, 6194–6202
14. Sorokin, A. V., Selyutina, A. A., Skabkin, M. A., Guryanov, S. G., Nazimov, I. V., Richard, C., Th'ng, J., Yau, J., Sorensen, P. H., Ovchinnikov, L. P., and Evdokimova, V. (2005) *EMBO J.* **24**, 3602–3612
15. Kuwano, M., Oda, Y., Izumi, H., Yang, S. J., Uchiumi, T., Iwamoto, Y., Toi, M., Fujii, T., Yamana, H., Kinoshita, H., Kamura, T., Tsuneyoshi, M., Yasumoto, K., and Kohno, K. (2004) *Mol. Cancer Ther.* **3**, 1485–1492
16. Torigoe, T., Izumi, H., Ishiguchi, H., Yoshida, Y., Tanabe, M., Yoshida, T., Igarashi, T., Niina, I., Wakasugi, T., Imaizumi, T., Momii, Y., Kuwano, M., and Kohno, K. (2005) *Curr. Med. Chem. Anticancer Agents* **5**, 15–27
17. Shibahara, K., Uchiumi, T., Fukuda, T., Kura, S., Tominaga, Y., Maehara, Y., Kohno, K., Nakabeppu, Y., Tsuzuki, T., and Kuwano, M. (2004) *Cancer Sci.* **95**, 348–353
18. Yoshida, S., Ohbo, K., Takakura, A., Takebayashi, H., Okada, T., Abe, K., and Nabeshima, Y. (2001) *Dev. Biol.* **240**, 517–530
19. Ohga, T., Koike, K., Ono, M., Makino, Y., Itagaki, Y., Tanimoto, M., Kuwano, M., and Kohno, K. (1996) *Cancer Res.* **56**, 4224–4228
20. Fleming, A., and Copp, A. J. (2000) *Hum. Mol. Genet.* **9**, 575–581
21. Harris, M. J., and Juriloff, D. M. (1999) *Teratology* **60**, 292–305
22. Ruzanov, P. V., Evdokimova, V. M., Korneeva, N. L., Hershey, J. W., and Ovchinnikov, L. P. (1999) *J. Cell Sci.* **112**, 3487–3496
23. Chen, C. Y., Gherzi, R., Andersen, J. S., Gaietta, G., Jurchott, K., Royer, H. D., Mann, M., and Karin, M. (2000) *Genes Dev.* **14**, 1236–1248
24. Lu, Z. H., Books, J. T., and Ley, T. J. (2005) *Mol. Cell. Biol.* **25**, 4625–4637
25. Juriloff, D. M., and Harris, M. J. (2000) *Hum. Mol. Genet.* **9**, 993–1000
26. Harris, M. J., and Juriloff, D. M. (1997) *Teratology* **56**, 177–187
27. Matsumoto, K., Tanaka, K. J., and Tsujimoto, M. (2005) *Mol. Cell. Biol.* **25**, 1779–1792
28. Skabkin, M. A., Kiselyova, O. I., Chernov, K. G., Sorokin, A. V., Dubrovin, E. V., Yaminsky, I. V., Vasiliev, V. D., and Ovchinnikov, L. P. (2004) *Nucleic Acids Res.* **32**, 5621–5635
29. Evdokimova, V. M., and Ovchinnikov, L. P. (1999) *Int. J. Biochem. Cell Biol.* **31**, 139–149
30. Huttelmaier, S., Zenklusen, D., Lederer, M., Dictenberg, J., Lorenz, M., Meng, X., Bassell, G. J., Condeelis, J., and Singer, R. H. (2005) *Nature* **438**, 512–515
31. Robinson, D. N., and Spudich, J. A. (2004) *Curr. Opin. Cell Biol.* **16**, 182–188
32. Jurchott, K., Bergmann, S., Stein, U., Walther, W., Janz, M., Manni, I., Piaggio, G., Fietze, E., Dietel, M., and Royer, H. D. (2003) *J. Biol. Chem.* **278**, 27988–27996
33. Swamynathan, S. K., Varma, B. R., Weber, K. T., and Guntaka, R. V. (2002) *Biochem. Biophys. Res. Commun.* **296**, 451–457
34. Bergmann, S., Royer-Pokora, B., Fietze, E., Jurchott, K., Hildebrandt, B., Trost, D., Leenders, F., Claude, J. C., Theuring, F., Bargou, R., Dietel, M., and Royer, H. D. (2005) *Cancer Res.* **65**, 4078–4087
35. Sutherland, B. W., Kucab, J., Wu, J., Lee, C., Cheang, M. C., Yorida, E., Turbin, D., Dedhar, S., Nelson, C., Pollak, M., Leighton Grimes, H., Miller, K., Badve, S., Huntsman, D., Blake-Gilks, C., Chen, M., Pallen, C. J., and Dunn, S. E. (2005) *Oncogene* **24**, 4281–4292
36. Evdokimova, V., Ruzanov, P., Anglesio, M. S., Sorokin, A. V., Ovchinnikov, L. P., Buckley, J., Triche, T. J., Sonenberg, N., and Sorensen, P. H. (2006) *Mol. Cell. Biol.* **26**, 277–292
37. Hay, N., and Sonenberg, N. (2004) *Genes Dev.* **18**, 1926–1945
38. Nekrasov, M. P., Ivshina, M. P., Chernov, K. G., Kovrigina, E. A., Evdokimova, V. M., Thomas, A. A., Hershey, J. W., and Ovchinnikov, L. P. (2003) *J. Biol. Chem.* **278**, 13936–13943
39. Bader, A. G., Felts, K. A., Jiang, N., Chang, H. W., and Vogt, P. K. (2003) *Proc. Natl. Acad. Sci. U. S. A.* **100**, 12384–12389
40. Bader, A. G., and Vogt, P. K. (2005) *Mol. Cell. Biol.* **25**, 2095–2106
41. Chang, Y. W., and Traugh, J. A. (1997) *J. Biol. Chem.* **272**, 28252–28257
42. Traugh, J. A. (2001) *Prog. Mol. Subcell. Biol.* **26**, 33–48
43. Edmonds, B. T., Wyckoff, J., Yeung, Y. G., Wang, Y., Stanley, E. R., Jones, J., Segall, J., and Condeelis, J. (1996) *J. Cell Sci.* **109**, 2705–2714
44. Gross, S. R., and Kinzy, T. G. (2005) *Nat. Struct. Mol. Biol.* **12**, 772–778

Available online at www.sciencedirect.com
SCIENCE DIRECT
ELSEVIER
Cancer Letters 234 (2006) 73–80
CANCER Letters
www.elsevier.com/locate/canlet

Mini review

Functional SNPs of the breast cancer resistance protein - therapeutic effects and inhibitor development

Kae Yanase [a,b], Satomi Tsukahara [b], Junko Mitsuhashi [a,b], Yoshikazu Sugimoto [a,b,*]

[a] *Department of Chemotherapy, Kyoritsu University of Pharmacy, 1-5-30 Shibakoen, Minato-ku, Tokyo 105-8512, Japan*
[b] *Cancer Chemotherapy Center, Japanese Foundation for Cancer Research, 3-10-6 Ariake, Koto-ku, Tokyo 135-8550, Japan*

Received 31 March 2005; accepted 20 April 2005

Abstract

Breast cancer resistance protein (BCRP) is a half-molecule ATP-binding cassette transporter that pumps out various anticancer agents such as 7-ethyl-10-hydroxycamptothecin, topotecan and mitoxantrone. We have previously identified three polymorphisms within the *BCRP* gene, G34A (substituting Met for Val-12), C376T (substituting a stop codon for Gln-126) and C421A (substituting Lys for Gln-141). C421A *BCRP*-transfected murine fibroblast PA317 cells showed markedly decreased protein expression and low-level drug resistance when compared with wild-type *BCRP*-transfected cells. In contrast, G34A *BCRP*-transfected PA317 cells showed a similar protein expression and drug resistance profile to wild-type. The C376T polymorphism would be expected to have a considerable impact as active BCRP protein will not be expressed from a T376 allele. Hence, people with C376T and/or C421A polymorphisms may express low levels of BCRP, resulting in hypersensitivity of normal cells to BCRP-substrate anticancer agents.

Estrogens, estrone and 17β-estradiol, were previously found to restore drug sensitivity levels in *BCRP*-transduced cells by increasing the cellular accumulation of anticancer agents. BCRP transports sulfated estrogens but not free estrogens and in a series of screening experiments for synthesized and natural estrogenic compounds, several tamoxifen derivatives and phytoestrogens/flavonoids were identified that effectively circumvent BCRP-mediated drug resistance. The kinase inhibitors gefitinib and imatinib mesylate also interact with BCRP. Gefitinib, an inhibitor of epidermal growth factor receptor-tyrosine kinase, inhibits its transporter function and reverses BCRP-mediated drug resistance both *in vitro* and *in vivo*. *BCRP*-transfected human epidermoid carcinoma A431 cells and *BCRP*-transfected human non-small cell lung cancer PC-9 cells show gefitinib resistance. Imatinib, an inhibitor of BCR-ABL tyrosine kinase, also inhibits BCRP-mediated drug transport. Hence, both functional SNPs and inhibitors of BCRP reduce its transporter function and thus modulate substrate pharmacokinetics and pharmacodynamics.

Keywords: ABCG2; Drug resistance; ABC transporter

1. Introduction

P-glycoprotein, MRP1 and BCRP are members of the ABC transporters that are involved in multidrug resistance [1–6]. These factors pump out various structurally unrelated chemotherapeutic agents in an energy-dependent manner and reduce their cytotoxic effects. BCRP, also known an ABCG2, is a half-

Abbreviations MRP, multidrug resistance-associated protein; BCRP, breast cancer resistance protein; ABC, ATP-binding cassette; SN-38, 7-ethyl-10-hydroxycamptothecin; MXR, mitoxantrone; SNPs, single-nucleotide polymorphisms.

* Corresponding author. Address: Department of Chemotherapy, Kyoritsu University of Pharmacy, 1-5-30 Shibakoen, Minato-ku, Tokyo 105-8512, Japan. Tel.: +81 3 5400 2670; fax: +81 3 5400 2669.
E-mail address: sugimoto-ys@kyoritsu-ph.ac.jp (Y. Sugimoto).

0304-3835/$ - see front matter © 2005 Elsevier Ireland Ltd. All rights reserved.
doi:10.1016/j.canlet.2005.04.039

molecule ABC transporter containing 655 amino acids that has an ATP-binding domain and a transmembrane domain [4–6]. BCRP functions as a homodimer and confers resistance to anticancer agents such as SN-38, topotecan and MXR [7–11]. BCRP is widely expressed in normal cells and tissues, such as capillary endothelial cells, hematopoietic stem cells, the maternal-fetal barrier of the placenta and the blood-brain barrier [12–14]. This suggests that BCRP plays a protective role against xenobiotics and their metabolites. The apical localization of BCRP in the intestinal epithelium and the bile canalicular membrane indicates that it plays an important role in preventing intestinal absorption and in mediating hepatobiliary excretion of its substrates [12]. In this way, BCRP restricts the bioavailability of orally administered BCRP-substrate agents. A dual inhibitor of BCRP and P-glycoprotein, GF120918, has been shown to increase the oral bioavailability of topotecan through the inhibition of BCRP function [15,16]. In addition, a recent report has shown that BCRP is highly expressed in the mammary glands of mice, cows and humans during lactation and that it is responsible for the active secretion of various substrates [17].

Recently, the study of SNPs has progressed rapidly and generated remarkable findings and some SNPs have been shown to affect both the expression and function of their gene products. In particular, SNPs of drug-metabolizing enzymes and drug transporters have been studied extensively and some have been shown to affect the pharmacokinetics and pharmacodynamics of anticancer agents. Cytochrome P450 (CYP) 2C8 is the principal enzyme responsible for the metabolism of the anticancer drug paclitaxel. A *CYP2C8*3* variant, containing the two amino acid substitutions R139K and K399R, in exons 3 and 8, was previously shown to be defective in paclitaxel metabolism [18]. SN-38 is detoxified by conjugation to SN-38-glucuronide by the UDP-glucronosyltransferase (UGT) 1A1 enzyme [19]. Significantly, a *UGT1A1*28* variant, containing a 2-bp insertion (TA) in the TATA box within the gene promoter, was found to be significantly related to the reduced expression of UGT1A1 and the increased bioavailability of SN-38 [20]. A C3435T SNP in exon 26 of the *MDR1* P-glycoprotein gene was elucidated as the first functional polymorphism of its type in ABC transporters and shown to be closely associated with low expression levels of P-glycoprotein and high plasma levels of digoxin [21]. Another SNP within the *MDR1* gene, C1236T, has also been associated with increased exposure to SN-38 and its prodrug irinotecan [22]. In the following chapter, we describe the functional SNPs within the *BCRP* gene that have been identified by our laboratory and by other groups.

2. The effects of SNPs on BCRP expression and function

2.1. C421A (Q141K) BCRP SNP

We have previously identified three variant *BCRP* cDNAs, containing the substitutions G34A (V12M), C421A (Q141K) and a 944-949 deletion lacking Ala-315 and Thr-316 (Δ315-6) [23]. The G34A and C421A substitutions are SNPs whereas the 944–949 deletion is a splicing variant. We have subsequently found that C421A *BCRP*-transfected murine fibroblast PA317 (PA/Q141K) cells show markedly decreased exogenous protein expression and also a low-level of drug resistance when normalized to wild-type *BCRP*-transfected (PA/WT) cells (Fig. 1 and Table 1). In addition, both G34A *BCRP*-transfected PA317 (PA/V12M) cells and 944–949-deleted *BCRP*-transfected PA317 (PA/Δ315-6) cells showed either similar or marginally lower protein expression and drug resistance levels compared to PA/WT cells (Fig. 1 and Table 1). We had already shown in our previous study that the intracellular topotecan accumulation in PA/Q141K cells was higher than in other *BCRP* transfectants [23].

Kondo et al. have also reported low Q141K-BCRP protein expression levels using adenovirus-mediated gene transfection [24]. In addition, Kobayashi et al. examined BCRP protein expression in Japanese placental samples, and found that its levels were significantly lower in A421 homozygotes than in samples containing wild-type C421 alleles and that heterozygotes had intermediate levels of expression [25]. In contrast however, Zamber et al. reported that no significant correlation between the C421A variant and BCRP expression was observed in human intestinal samples [26]. The possible significance of the C421A-*BCRP* SNP on the pharmacokinetics of diflomotecan, a new camptothecin derivative anticancer agent, has also been evaluated in a phase I study [27]. In this trial, five patients who were heterozygous for the A421 allele,

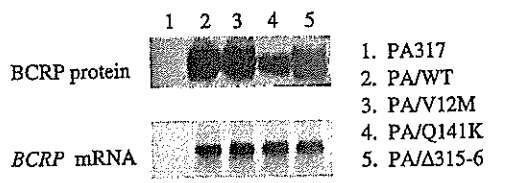

Fig. 1. Expression of BCRP protein and *BCRP* mRNA in PA317 cells transfected with *BCRP* variants.

Table 1
Drug sensitivities of *BCRP*-transfected PA317 cells

Cells	IC_{50} (ng/ml)		
	SN-38	Topotecan	MXR
PA317	2.5	0.060	17
PA/WT	98	0.58	>200
PA/V12M	98	0.63	>200
PA/Q141K	30	0.25	100
PA/Δ315-6	55	0.42	190

Cells were cultured for 5 days in the absence or presence of increasing concentrations of the indicated anticancer agents. Cell numbers were determined with a Coulter counter and IC_{50} values were calculated.

showed plasma levels of diflomotecan, after intravenous administration, that were 299% ($P=0.015$) of the levels in 15 patients who were homozygous wild-type, with mean values of 138 ng h/mL mg^{-1} versus 46.1 ng h/mL mg^{-1}, respectively [27]. The findings of this clinical study also support our hypothesis that the expression levels and subsequent functions of the A421-*BCRP* allele are disrupted when compared to the wild-type C421 gene.

The C421A SNP occurs in the functionally important ATP-binding region between the Walker A and B motifs and results in substitution of the positively charged Lys residue for a neutral Gln residue. This may be associated with a greater susceptibility of the resulting BCRP protein (Q141K) to degradation [23]. In addition, Mizuarai et al. have also reported that ATPase activity levels in the membrane of C421A *BCRP*-transduced insect Sf9 cells were 1.3-fold lower than wild-type cells [28].

We previously examined the frequency of the C421A SNP in a normal Japanese population and found that 57/124 samples carried the A421 allele and that nine of these were homozygous for this polymorphism [23], indicating that some individuals possess the C421A polymorphic *BCRP* gene and express low amounts of the Q141K BCRP. C421A is therefore an important SNP because the allelic frequency of this variant differs greatly between diverse populations (Table 2). The C421A variant also appears to be very common in Asian populations, with reported allele frequencies of between 27 and 34% [23,25,29]. In contrast, this variant is rare in sub-Sahara African and in African American populations, with a frequency of <5% [25,29]. The frequency in Caucasian populations is approximately 10% [25,28–30].

2.2. C376T (Q126stop)-BCRP SNP

Another of the *BCRP* gene SNPs, C376T, substitutes a stop codon for Gln-126 (Q126stop), and was found in 3/124 of our general Japanese samples as a heterozygosity [23]. C376T was also detected previously in another report in 2/120 Japanese placental samples, again as a heterozygosity [25]. Although the frequency of the T376 allele is low, this variant would be expected to have a high impact as no active BCRP protein could be expressed from this gene. Stop SNPs have been reported in the *MRP2* gene, which is responsible for the hyperbilirubinemia of Dubin-Johnson syndrome, but are relatively rare and would usually be classified as naturally occurring base changes [31,32]. This C371T *BCRP* SNP is thus an important variant because of relatively high frequency (~1% in Japanese) as a stop SNP. Individuals with either the C376T and/or C421A SNPs may express low amounts of BCRP and this may result in hypersensitivity of normal cells to anticancer agents.

2.3. Additional BCRP SNPs

BCRP SNPs are summarized in Table 3 and include G34A, G151T, C376T, C421A, C458T, C496G, A616C, T623C, T742C, G1000T, T1291C, T1465C, A1768T and G1858A, which all cause amino acid changes. Among these, in addition to C376T and C421A, only a few have been examined in association with protein expression levels and the function of BCRP. Mizuarai et al. reported that the G34A variant exhibits reduced drug resistance in polarized porcine kidney epithelial LLC-PK1 cells along with increased intracellular drug accumulation [28]. However, in our

Table 2
Frequency of the C421A *BCRP* allele among different ethnic populations

Population	N	Genotype		Allele frequency[a] (%)	Ref.
		C/A	A/A		
Asian (Japanese)	124	48	9	27	[23]
	120	45	14	30	[25]
(Han Chinese)	95	43	11	34	[29]
Caucasian	150	25	4	11	[25]
	150	22	2	9	[28]
(American)	88	19	1	12	[29]
(European)	84	14	2	11	[29]
(Swedish)	60	10	1	10	[30]
African (sub-Saharan)	938	14	1	1	[29]
African-American	94	8	1	5	[29]
	150	5	1	2	[25]

Abbreviations: *N*, number of patients studied; C/A, heterozygous frequency; A/A, homozygous variant frequency; Ref., reference.
[a] Data are given as the relative frequency of variant alleles.

Table 3
SNPs within the *BCRP* gene

Variation	Region	Effect	Domain
A-1379G	5′-flanking (promoter)	–	
Δ-654–651	5′-flanking (promoter)	–	
G-286C	5′-flanking (promoter)	–	
T-476C	Exon 1 (5′-UTR)	–	
Δ-235A	Exon 1 (5′-UTR)	–	
A-113G	Exon 1 (5′-UTR)	–	
A-29G	Exon 1 (5′-UTR)	–	
G34A	Exon 2	V12M	N-terminal
T114C	Exon 2	No change	N-terminal
G151T	Exon 2	G51C	N-terminal
C369T	Exon 4	No change	NBD
C376T	Exon 4	Q126stop	NBD
C421A	Exon 5	Q141K	NBD
C458T	Exon 5	T153M	NBD
C474T	Exon 5	No change	NBD
C496G	Exon 5	Q166E	NBD
A564G	Exon 6	No change	NBD
A616C	Exon 6	I206L	NBD
T623C	Exon 6	F208S	NBD
T742C	Exon 7	S248P	Linker
G1000T	Exon 9	E334stop	Linker
G1098A	Exon 9	No change	Linker
T1291C	Exon 11	F431L	TMD
A1425G	Exon 12	No change	TMD
T1465C	Exon 12	F489L	TMD
A1768T	Exon 15	N590Y	TMD
G1858A	Exon 16	D620N	TMD
G2237T	Exon 16 (3′-UTR)	–	
G2393T	Exon 16 (3′-UTR)	–	

Abbreviations: UTR, untranslated region; NBD, nucleotide-binding domain; TMD, transmembrane domain.

previous study we showed a different outcome [23]. Further studies of *BCRP* SNPs and their roles in the expression and/or function of this protein would provide a fuller picture of its genetic regulation. In addition, these findings may be essential for our complete understanding of the pharmacological activities and pharmacokinetic profiles of BCRP-substrate anticancer agents.

3. BCRP inhibitors

BCRP inhibitors have two important clinical implications. First, they may overcome BCRP-mediated drug resistance in tumor cells. Second, they may modulate the pharmacokinetics and pharmacodynamics of BCRP-substrate agents in normal tissues and consequently increase the toxicity of specific anticancer agents. Various compounds have been found to reverse drug resistance through the inhibition of BCRP function [33–36]. In this chapter, we summarize the BCRP inhibitors identified by our laboratory and also by other groups (Table 4). The chemical structures of some of these inhibitors are shown in Fig. 2.

3.1. Estrogens and their metabolites

We were the first laboratory to identify estrogens as BCRP inhibitors and show that estrone and 17β-estradiol can restore drug sensitivity in *BCRP*-transduced human myelogenous leukemia K562 (K562/BCRP) cells [37]. These agents showed only a marginal growth-inhibitory effect on either K562/BCRP or parental K562 cells and increased the cellular accumulation of topotecan in K562/BCRP cells, but not in K562 cells. BCRP is highly expressed in the syncytiotrophoblasts of the placenta that synthesize and secrete these estrogens [12]. Therefore, we first

Table 4
BCRP inhibitors and substrates

Compound	Reference
1. Anticancer agents	
SN-38[a]	[8,11]
Topotecan[a]	[8,9]
MXR[a]	[5,6]
Flavopiridol[a]	[53]
Gefitinib	[46–49]
Imatinib mesylate	[50,51]
CI1033	[52]
Methotrexate polyglutamate[a]	[39,54]
2. Steroid hormones	
Estrone, Estradiol, Estriol	[37]
3. Sulfated steroids	
Estrone sulfate[a], Estradiol sulfate[a]	[38–40]
Dehydroepiandrosterone sulfate[a]	[40]
4. Synthesized estrogens	
Diethylstilbestrol	[41]
5. Anti-estrogens	
Tamoxifen, Toremifene, TAG-139	[41]
6. Flavonoids	
Genistein[a], Naringenin, Acacetin, Kaempferol, Naringenin-7-glucoside	[42]
7. Others	
Hoechst 33342[a]	[55]
Fumitremorgin C	[34]
GF120918	[33]
Novobiocin	[35,36]

[a] Compounds that are transported by BCRP (BCRP substrates).

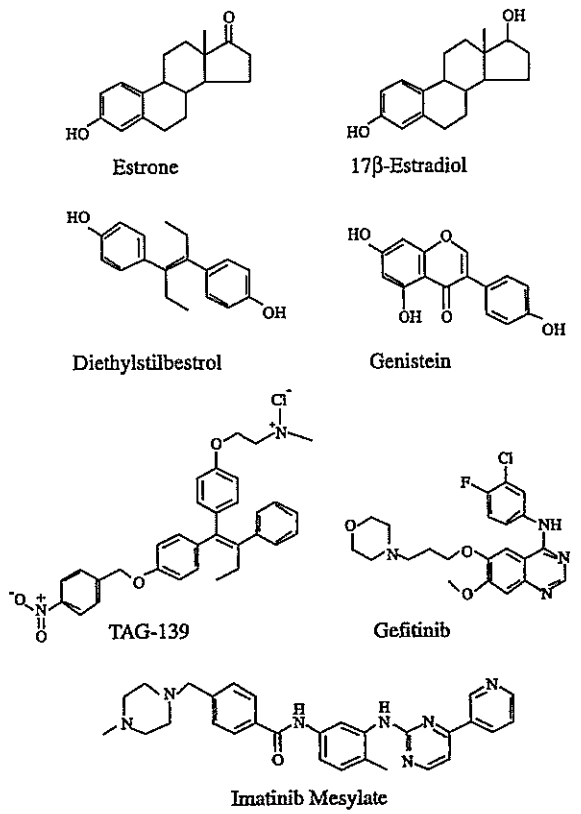

Fig. 2. Chemical structures of BCRP inhibitors.

hypothesized that these estrogens would be physiological substrates of BCRP and be transported by BCRP. To clarify this, we performed a transcellular transport assay using *BCRP*-transduced LLC-PK1 (LLC/BCRP) cells, in which exogenous BCRP is expressed in the apical membranes [38]. In this assay, excretion of ^{3}H-labeled estrone and 17β-estradiol was high and reabsorption was low in BCRP-expressing cells. However, thin layer chromatography analysis demonstrated an increased excretion of estrone sulfate and 17β-estradiol sulfate, but not estrone or 17β-estradiol, in LLC/BCRP cells. Fumitremorgin C completely inhibited the increased excretion of sulfated estrogens across the apical membrane. Moreover, the conversion of estrogens into their sulfate conjugates was similar between LLC/BCRP and LLC-PK1 cells, suggesting that the increased excretion of estrone sulfate was attributable to BCRP-mediated transport. The BCRP- and ATP-dependent uptake of ^{3}H-labeled estrone sulfate, but neither estrone nor 17β-estradiol, was also observed in membrane vesicles from K562/BCRP cells. Additionally, SN-38 and fumitremorgin C both suppressed the transport of estrone sulfate in membrane vesicles from K562/BCRP cells. Our findings thus suggest that BCRP does not transport either free estrone or 17β-estradiol but exports the corresponding sulfate conjugates of these estrogens [38–40].

3.2. Estrogen agonists and antagonists

Estrogen agonists, antagonists and their derivatives have been also evaluated in this laboratory for potential BCRP-reversing activities [41]. Among the commercially available compounds that we tested, diethylstilbestrol showed the strongest BCRP-reversing activity and was found to increase the cellular accumulation of topotecan and reverse resistance to SN-38 and MXR in K562/BCRP cells, but show either marginal or no effects in parental K562 cells [41]. In contrast, neither tamoxifen nor toremifene have much effect on increasing topotecan uptake in K562/BCRP cells. In our screening with various tamoxifen derivatives for BCRP inhibitors, TAG-139 was identified as a strong candidate [41]. Reversal of SN-38 and MXR resistance in K562/BCRP cells by TAG-139 was 5-fold stronger than estrone. Interestingly, the dose-dependent characteristics of drug resistance reversal by TAG-139 and estrone were very similar, suggesting that tamoxifen derivatives and estrone interact with the same binding site of BCRP [41].

3.3. Phytoestrogens/flavonoids

Some flavonoids that show weak estrogenic activities are called phytoestrogens. We have shown that these phytoestrogens/flavonoids, such as genistein, naringenin, acacetin and kaempferol, potentiate the cytotoxicity of SN-38 and MXR in K562/BCRP cells [42]. Some glycosylated flavonoids, such as naringenin-7-glucoside, are also effective inhibitors of BCRP and showed marginal effects on the drug sensitivity of K562 cells. Genistein and naringenin did not reverse either P-glycoprotein-mediated vincristine resistance or MRP1-mediated etoposide resistance but increased the cellular accumulation of topotecan in K562/BCRP cells. K562/BCRP cells also accumulated less ^{3}H-labeled genistein than K562 cells. In addition, the excretion of ^{3}H-labeled genistein was greater in LLC/BCRP cells than that in parental LLC-PK1 cells. Fumitremorgin C abolished the increased excretion of ^{3}H-labeled genistein in LLC/BCRP cells and thin layer chromatography analysis revealed that genistein is transported in its native form but not in its metabolized form. These results suggest that genistein is among the natural substrates of BCRP and competitively inhibits the BCRP-mediated drug efflux [42].

3.4. Kinase inhibitors

Gefitinib is an orally active, selective epidermal growth factor receptor-tyrosine kinase inhibitor that is currently used in the treatment of patients with advanced non-small cell lung cancer [43,44]. Recently, the possible interaction of gefitinib with BCRP has been evaluated by this laboratory and others [45–49]. Gefitinib was found to reverse SN-38 resistance in K562/BCRP cells and *BCRP*-transduced murine lymphocytic leukemia P388 cells, but not in the parental cells [46]. Furthermore, gefitinib increases the intracellular accumulation of topotecan in K562/BCRP cells and also suppresses the ATP-dependent transport of estrone sulfate in membrane vesicles from these cells. Additionally, the combination of gefitinib with irinotecan was shown to result in the markedly enhanced antitumor activity of irinotecan in multiple tumor models [46]. These results suggest that gefitinib inhibits the transporter function of BCRP and reverses BCRP-mediated drug resistance both in vitro and in vivo. Stewart et al. have also indicated that oral dosing of gefitinib significantly increases the oral bioavailability of irinotecan [47]. Furthermore, *BCRP*-transduced human epidermoid carcinoma A431 cells and *BCRP*-transduced human non-small cell lung cancer PC-9 cells acquired cellular resistance to gefitinib [46]. Elkind et al. have also reported that the expression of functional BCRP protects the A431 cells from the cytotoxic effects of gefitinib [49]. These findings strongly suggest that BCRP is one of the important determinants of gefitinib sensitivity.

Imatinib mesylate, an inhibitor of BCR-ABL tyrosine kinase, has been reported to reverse BCRP-mediated drug resistance [50,51]. Houghton et al. reported that imatinib significantly increase the accumulation of topotecan in the human osteosarcoma Saos2 cells expressing functional BCRP [50]. However, the overexpression of BCRP did not confer resistance to imatinib and the accumulation of ^{14}C-labeled imatinib was similar in Saos2 cells expressing either functional or non-functional BCRP. These results suggest that imatinib binds to BCRP and inhibits its function but that it is not a BCRP substrate [50]. In contrast, Burger et al. have reported that imatinib is in fact a substrate for BCRP [51] by demonstrating that the accumulation of imatinib is low in a BCRP-overexpressing subline, MCF7/MR. They also showed that Ko-143, a specific inhibitor of BCRP, increased the accumulation of imatinib in MCF7/MR cells [51]. Another potent tyrosine kinase inhibitor, CI1033, has also been shown to enhance the uptake and cytotoxicity of SN-38 and topotecan in *BCRP*-transfected cells [52]. CI1033 accumulation was diminished in BCRP-expressing cells, suggesting that it may be transported by BCRP [52].

4. Conclusions

There is great variation in the response of patients to cancer chemotherapy, in terms of both treatment efficacy and host toxicity. BCRP confers resistance to agents such as irinotecan, topotecan and MXR that are used in practical chemotherapy for a wide variety of cancers. BCRP expression in the normal tissues of cancer patients may also serve to reduce the adverse effects of these agents, such as hematological toxicity and digestive disorders. C376T and C421A SNPs within the *BCRP* gene were shown to be associated with low protein expression and increased sensitivity to BCRP-substrate anticancer agents. Hence, individuals with these SNPs may demonstrate a different bioavailability of irinotecan due to its decreased excretion, and consequent increased intracellular and plasma levels. Consequently, C376T and C421A SNPs might also be implicated in the side effects of irinotecan. Screening for such functional SNPs in cancer patients prior to chemotherapy may thus be useful for the prevention of serious side effects of anticancer agents.

BCRP was also shown to be associated with the excretion of sulfated estrogens and other sulfated compounds. Because BCRP is responsible for the excretion of several anticancer agents, the inhibition of its function may lead to the increased plasma levels of orally administered agents. It is possible that BCRP inhibitors alter the bioavailability of BCRP substrates. These effects might be manipulated to the advantage of clinicians by improving several aspects of chemotherapy such as reduction of the variability in exposure to orally administered topotecan and potentiation of the cytotoxic activity of irinotecan. In addition, unintentional side effects may be caused by modulation of the bioavailability of chemotherapeutics by BCRP inhibitors.

These findings indicate that functional SNPs and inhibitors of BCRP result in similar effects on the pharmacokinetics of BCRP-substrate agents. In clinical studies of BCRP-substrate anticancer agents (e.g. diflomotecan) and BCRP inhibitors (e.g. flavonoids), patients should therefore be evaluated according to their *BCRP* genotypes. Also, treatment regimens should be modified according to the SNP status of the patients to minimize unintentional side effects.

References

[1] M.M. Gottesman, C.A. Hrycyna, P.V. Schoenlein, U.A. Germann, I. Pastan, Genetic analysis of the multidrug transporter, Annu. Rev. Genet. 29 (1995) 607–649.

[2] C.J. Chen, J.E. Chin, K. Ueda, D.P. Clark, I. Pastan, M.M. Gottesman, et al., Internal duplication and homology with bacterial transport proteins in the *mdr1* (P-glycoprotein) gene from multidrug-resistant human cells, Cell 47 (1986) 381–389.

[3] S.P. Cole, G. Bhardwaj, J.H. Gerlach, J.E. Mackie, C.E. Grant, K.C. Almquist, et al., Overexpression of a transporter gene in a multidrug-resistant human lung cancer cell line, Science 258 (1992) 1650–1654.

[4] R. Allikmets, L. Schriml, A. Hutchinson, V. Romano-Spica, M. Dean, A human placenta-specific ATP-binding cassette gene (*ABCP*) on chromosome 4q22 that is involved in multidrug resistance, Cancer Res. 58 (1998) 5337–5339.

[5] L.A. Doyle, W. Yang, L.V. Abruzzo, T. Krogmann, Y. Gao, A.K. Rishi, et al., A multidrug resistance transporter from human MCF-7 breast cancer cells, Proc. Natl Acad. Sci. USA 95 (1998) 15665–15670.

[6] K. Miyake, L. Mickley, T. Litman, Z. Zhan, R. Robey, B. Cristensen, et al., Molecular cloning of cDNAs which is highly overexpressed in mitoxantrone-resistant cells: demonstration of homology to ABC transport genes, Cancer Res. 59 (1999) 8–13.

[7] K. Kage, S. Tsukahara, T. Sugiyama, S. Asada, E. Ishikawa, T. Tsuruo, et al., Dominant-negative inhibition of breast cancer resistance protein as drug efflux pump through the inhibition of S-S dependent homodimerization, Int. J. Cancer 97 (2002) 626–630.

[8] M. Maliepaard, M.A. van Gastelen, L.A. de Jong, D. Pluim, R.C. van Waardenburg, M.C. Ruevekamp-Helmers, et al., Overexpression of the *BCRP/MXR/ABCP* gene in a topotecan-selected ovarian tumor cell line, Cancer Res. 59 (1999) 4559–4563.

[9] J.D. Allen, R.F. Brinkhuis, J. Wijnholds, A.H. Schinkel, The mouse *Bcrp1/Mxr/Abcp* gene: amplification and overexpression in cell lines selected for resistance to topotecan, mitoxantrone, or doxorubicin, Cancer Res. 59 (1999) 4237–4241.

[10] C.H. Yang, E. Schneider, M.L. Kuo, E.L. Volk, E. Rocchi, Y.C. Chen, BCRP/MXR/ABCP expression in topotecan-resistant human breast carcinoma cells, Biochem. Pharmacol. 60 (2000) 831–837.

[11] S. Kawabata, M. Oka, K. Shiozawa, K. Tsukamoto, K. Nakatomi, H. Soda, et al., Breast cancer resistance protein directly confers SN-38 resistance of lung cancer cells, Biochem. Biophys. Res. Commun. 280 (2001) 1216–1223.

[12] M. Maliepaard, G.L. Scheffer, I.F. Faneyte, M.A. van Gastelen, A.C. Pijnenborg, A.H. Schinkel, et al., Subcellular localization and distribution of the breast cancer resistance protein transporter in normal human tissues, Cancer Res. 61 (2001) 3458–3464.

[13] S. Zhou, J.D. Schuetz, K.D. Bunting, A.M. Colapietro, J. Sampath, J.J. Morris, et al., The ABC transporter Bcrp1/ABCG2 is expressed in a wide variety of stem cells and is a molecular determinant of the side-population phenotype, Nat. Med. 7 (2001) 1028–1034.

[14] T. Eisenblatter, H.J. Galla, A new multidrug resistance protein at the blood-brain barrier, Biochem. Biophys. Res. Commun. 293 (2002) 1273–1278.

[15] J.W. Jonker, J.W. Smit, R.F. Brinkhuis, M. Maliepaard, J.H. Beijnen, J.H. Schellens, et al., Role of breast cancer resistance protein in the bioavailability and fetal penetration of topotecan, J. Natl Cancer Inst. 92 (2000) 1651–1656.

[16] C.M. Kruijtzer, J.H. Beijnen, H. Rosing, W.W. ten Bokkel Huinink, M. Schot, R.C. Jewell, et al., Increased oral bioavailability of topotecan in combination with the breast cancer resistance protein and P-glycoprotein inhibitor GF120918, J. Clin. Oncol. 20 (2002) 2943–2950.

[17] J.W. Jonker, G. Merino, S. Musters, A.E. van Herwaarden, E. Bolscher, E. Wagenaar, et al., The breast cancer resistance protein BCRP (ABCG2) concentrates drugs and carcinogenic xenotoxins into milk, Nat. Med. 11 (2005) 127–129.

[18] D. Dai, D.C. Zeldin, J.A. Blaisdell, B. Chanas, S.J. Coulter, B.I. Ghanayem, et al., Polymorphisms in human CYP2C8 decrease metabolism of the anticancer drug paclitaxel and arachidonic acid, Pharmacogenetics 11 (2001) 597–607.

[19] L. Iyer, C.D. King, P.F. Whitington, M.D. Green, S.K. Roy, T.R. Tephly, et al., Genetic predisposition to the metabolism of irinotecan (CPT-11). Role of uridine diphosphate glucuronosyltransferase isoform 1A1 in the glucuronidation of its active metabolite (SN-38) in human liver microsomes, J. Clin. Invest. 101 (1998) 847–854.

[20] Y. Ando, H. Saka, M. Ando, T. Sawa, K. Muro, H. Ueoka, et al., Polymorphisms of UDP-glucuronosyltransferase gene and irinotecan toxicity: a pharmacogenetic analysis, Cancer Res. 60 (2000) 6921–6926.

[21] S. Hoffmeyer, O. Burk, O. von Richter, H.P. Arnold, J. Brockmoller, A. Johne, et al., Functional polymorphisms of the human multidrug-resistance gene: multiple sequence variations and correlation of one allele with P-glycoprotein expression and activity in vivo, Proc. Natl Acad. Sci. USA 97 (2000) 3473–3478.

[22] R.H. Mathijssen, S. Marsh, M.O. Karlsson, R. Xie, S.D. Baker, J. Verweij, et al., Irinotecan pathway genotype analysis to predict pharmacokinetics, Clin. Cancer Res. 9 (2003) 3246–3253.

[23] Y. Imai, M. Nakane, K. Kage, S. Tsukahara, E. Ishikawa, T. Tsuruo, et al., C421A polymorphism in the human breast cancer resistance protein gene is associated with low expression of Q141K protein and low-level drug resistance, Mol. Cancer Ther. 1 (2002) 611–616.

[24] C. Kondo, H. Suzuki, M. Itoda, S. Ozawa, J. Sawada, D. Kobayashi, et al., Functional analysis of SNPs variants of BCRP/ABCG2, Pharm. Res. 21 (2004) 1895–1903.

[25] D. Kobayashi, I. Ieiri, T. Hirota, H. Takane, S. Maegawa, J. Kigawa, et al., Functional assessment of abcg2 (bcrp) gene polymorphisms to protein expression in human placenta, Drug Metab. Dispos. 33 (2005) 94–101.

[26] C.P. Zamber, J.K. Lamba, K. Yasuda, J. Farnum, K. Thummel, J.D. Schuetz, et al., Natural allelic variants of breast cancer resistance protein (BCRP) and their relationship to BCRP expression in human intestine, Pharmacogenetics 13 (2003) 19–28.

[27] A. Sparreboom, H. Gelderblom, S. Marsh, R. Ahluwalia, R. Obach, P. Principe, et al., Diflomotecan pharmacokinetics in relation to ABCG2 421C>A genotype, Clin. Pharmacol. Ther. 76 (2004) 38–44.

[28] S. Mizuarai, N. Aozasa, H. Kotani, Single nucleotide polymorphisms result in impaired membrane localization and reduced atpase activity in multidrug transporter ABCG2, Int. J. Cancer 109 (2004) 238–246.